universe

MDPI

Article

Gravitational Waves, μ Term and Leptogenesis from $B - L$ Higgs Inflation in Supergravity

Constantinos Pallis

Department of Physics, University of Cyprus, P.O. Box 20537, Nicosia 1678, Cyprus; cpallis@ucy.ac.cy

Received: 25 October 2017; Accepted: 15 December 2017; Published: 9 January 2018

Abstract: We consider a renormalizable extension of the minimal supersymmetric standard model endowed by an R and a gauged $B - L$ symmetry. The model incorporates chaotic inflation driven by a quartic potential, associated with the Higgs field which leads to a spontaneous breaking of $U(1)_{B-L}$, and yields possibly detectable gravitational waves. We employ quadratic Kähler potential with a prominent shift-symmetric part proportional to c_- and a tiny violation, proportional to c_+, included in a logarithm with prefactor $-N < 0$. An explanation of the μ term of the MSSM is also provided, consistently with the low energy phenomenology, under the condition that one related parameter in the superpotential is somewhat small. Baryogenesis occurs via non-thermal leptogenesis which is realized by the inflaton's decay to the lightest or next-to-lightest right-handed neutrino with masses lower than 1.8×10^{13} GeV. Our scenario can be confronted with the current data on the inflationary observables, the baryon asymmetry of the universe, the gravitino limit on the reheating temperature and the data on the neutrino oscillation parameters, for $0.012 \lesssim c_+/c_- \lesssim 1/N$ and gravitino as light as 1 TeV.

Keywords: cosmology; inflation; supersymmetric models

1. Introduction

One of the primary ideas, followed the introduction of inflation [1–3] as a solution to longstanding cosmological problems—such as the horizon, flatness and magnetic monopoles problems—was its connection with a phase transition related to the breakdown of a Grand Unified Theory (GUT) According to this economical and highly appealing scenario—called henceforth Higgs inflation (HI)—the inflaton may be identified with one particle involved in the Higgs sector [4–24] of a GUT model. In a series of recent papers [25,26] we established a novel type of GUT-scale, mainly, HI called kinetically modified non-Minimal HI. This term is coined in Reference [27,28] due to the fact that, in the non-Supersymmetric (SUSY) set-up, this inflationary model, based on the ϕ^4 power-law potential, employs not only a suitably selected non-minimal coupling to gravity $f_{\mathcal{R}} = 1 + c_+\phi^2$ but also a kinetic mixing of the form $f_{\rm K} = c_- f_{\mathcal{R}}^m$—cf. Reference [29–31]. The merits of this construction compared to the original (and certainly more predictive) model [4,5,32,33] of non-minimal inflation (nMI) defined for $f_{\rm K} = 1$ are basically two:

(i) For $m \geq 0$, the observables depend on the ratio $r_\pm = c_+/c_-$ and can be done excellently consistent with the *Planck* [34] and BICEP2/*Keck Array* [35] results. More specifically, all data taken by the BICEP2/*Keck Array* CMB polarization experiments up to and including the 2014 observing season (BK14) [35] seem to favor r's of order 0.01 since the output of the analysis is

$$r = 0.028^{+0.026}_{-0.025} \;\Rightarrow\; 0.003 \lesssim r \lesssim 0.054 \; at \; 68\% \; c.l. \tag{1}$$

(ii) The resulting theory respects the perturbative unitarity [36–38] up to the Planck scale for $r_\pm \leq 1$ and m of order unity.

In the SUSY—which means Supergravity (SUGRA)—framework the two ingredients necessary to achieve this kind of nMI, i.e., the non-minimal kinetic mixing and coupling to gravity, originate from the same function, the Kähler potential, and the set-up becomes much more attractive. Actually, the non-minimal kinetic mixing and gravitational coupling of the inflaton can be elegantly realized introducing an approximate shift symmetry [25,29–31,39–48]. Namely, the constants c_- and c_+ introduced above can be interpreted as the coefficients of the principal shift-symmetric term (c_-) and its violation (c_+) in the Kähler potentials K. Allowing also for a variation of the coefficients of the logarithms appearing in the K's we end up with the most general form of these models analyzed in Reference [26].

Here, we firstly single out the most promising models from those investigated in Reference [26], employing as a guiding principle the consistency of the expansion of the K's in powers of the various fields. Namely, as we mention in Reference [26], $m = 0$ and $m = 1$ are the two most natural choices since they require just quadratic terms in some of the K's considered. From these two choices the one with $m = 1$ is privileged since it ensures r within Equation (1) with central value for the spectral index n_s. Armed with the novel stabilization mechanisms for the non-inflaton accompanied field—recently proposed in the context of the Starobinsky-type inflation [49–51] too—we concentrate here on K's including exclusively quadratic terms with $m = 1$. The embedding of the selected models in a complete framework is the second aim of this paper. Indeed, a complete inflationary model should specify the transition to the radiation domination, explain the origin of the observed baryon asymmetry of the universe (BAU) [52,53] and also, yield the minimal supersymmetric standard model (MSSM) as low energy theory. Although this task was carried out for similar models—see, e.g., References [12,13,54,55]—it would be certainly interesting to try to adapt it to the present set-up. Further restrictions are induced from this procedure.

A GUT based on $G_{B-L} = G_{\rm SM} \times U(1)_{B-L}$, where $G_{\rm SM} = SU(3)_{\rm C} \times SU(2)_{\rm L} \times U(1)_Y$ is the gauge group of the standard model and B and L denote the baryon and lepton number respectively, consists [25,26,48] a conveniently simple framework which allows us to exemplify our proposal. Actually, this is a minimal extension of the MSSM which is obtained by promoting the already existing $U(1)_{B-L}$ global symmetry to a local one. The Higgs fields which cause the spontaneous breaking of the G_{B-L} symmetry to $G_{\rm SM}$ can naturally play the role of inflaton. This breaking provides large Majorana masses to the right-handed neutrinos, N_i^c, whose the presence is imperative in order to cancel the gauge anomalies and generate the tiny neutrino masses via the seesaw mechanism. Furthermore, the out-of-equilibrium decay of the N_i^c's provides us with an explanation of the observed BAU [56] via non-thermal leptogenesis (nTL) [57–59] consistently with the gravitino ($\widetilde{G}$) constraint [60–69] and the data [70–72] on the neutrino oscillation parameters. As a consequence, finally, of an adopted global R symmetry, the parameter μ appearing in the mixing term between the two electroweak Higgs fields in the superpotential of MSSM is explained as in References [54,73] via the vacuum expectation value (v.e.v) of the non-inflaton accompanying field, provided that the relevant coupling constant is rather suppressed.

Below, we present the particle content, the superpotential and the possible Kähler potentials which define our model in Section 2. In Section 3 we describe the inflationary potential, derive the inflationary observables and confront them with observations. Section 4 is devoted to the resolution of the μ problem of MSSM. In Section 5 we analyze the scenario of nTL exhibiting the relevant constraints and restricting further the parameters. Our conclusions are summarized in Section 6. Throughout the text, the subscript of type $,z$ denotes derivation with respect to (wrt) the field z and charge conjugation is denoted by a star. Unless otherwise stated, we use units where $m_{\rm P} = 2.433 \times 10^{18}$ GeV is taken unity.

2. Model Description

We focus on an extension of MSSM invariant under the gauge group G_{B-L}. Besides the MSSM particle content, the model is augmented by six superfields: a gauge singlet S, three N_i^c's, and a pair of Higgs fields Φ and $\bar{\Phi}$ which break $U(1)_{B-L}$. In addition to the local symmetry, the model possesses also the baryon and lepton number symmetries and a nonanomalous R symmetry $U(1)_R$. The charge

assignments under these symmetries of the various matter and Higgs superfields are listed in Table 1. We below present the superpotential (Section 2.1) and (some of) the Kähler potentials (Section 2.2) which give rise to our inflationary scenario.

Table 1. The representations under G_{B-L} and the extra global charges of the superfields of our model.

Superfields	Representations Under G_{B-L}	Global Symmetries		
		R	B	L
Matter Fields				
e_i^c	$(\mathbf{1},\mathbf{1},1,1)$	1	0	-1
N_i^c	$(\mathbf{1},\mathbf{1},0,1)$	1	0	-1
L_i	$(\mathbf{1},\mathbf{2},-1/2,-1)$	1	0	1
u_i^c	$(\mathbf{3},\mathbf{1},-2/3,-1/3)$	1	$-1/3$	0
d_i^c	$(\mathbf{3},\mathbf{1},1/3,-1/3)$	1	$-1/3$	0
Q_i	$(\bar{\mathbf{3}},\mathbf{2},1/6,1/3)$	1	1/3	0
Higgs Fields				
H_d	$(\mathbf{1},\mathbf{2},-1/2,0)$	0	0	0
H_u	$(\mathbf{1},\mathbf{2},1/2,0)$	0	0	0
S	$(\mathbf{1},\mathbf{1},0,0)$	2	0	0
Φ	$(\mathbf{1},\mathbf{1},0,2)$	0	0	-2
$\bar{\Phi}$	$(\mathbf{1},\mathbf{1},0,-2)$	0	0	2

2.1. Superpotential

The superpotential of our model naturally splits into two parts:

$$W = W_{\rm MSSM} + W_{\rm HI}, \tag{2}$$

where

(a) $W_{\rm MSSM}$ is the part of W which contains the usual terms—except for the μ term—of MSSM, supplemented by Yukawa interactions among the left-handed leptons (L_i) and N_i^c:

$$W_{\rm MSSM} = h_{ijD} d_i^c Q_j H_d + h_{ijU} u_i^c Q_j H_u + h_{ijE} e_i^c L_j H_d + h_{ijN} N_i^c L_j H_u. \tag{3a}$$

Here the ith generation $SU(2)_{\rm L}$ doublet left-handed quark and lepton superfields are denoted by Q_i and L_i respectively, whereas the $SU(2)_{\rm L}$ singlet antiquark [antilepton] superfields by u_i^c and ${d_i}^c$ [e_i^c and N_i^c] respectively. The electroweak Higgs superfields which couple to the up [down] quark superfields are denoted by H_u [H_d].

(b) $W_{\rm HI}$ is the part of W which is relevant for HI, the generation of the μ term of MSSM and the Majorana masses for N_i^c's. It takes the form

$$W_{\rm HI} = \lambda S \left(\bar{\Phi}\Phi - M^2/4 \right) + \lambda_\mu S H_u H_d + \lambda_{iN^c} \bar{\Phi} N_i^{c2}. \tag{3b}$$

The imposed $U(1)_R$ symmetry ensures the linearity of $W_{\rm HI}$ wrt S. This fact allows us to isolate easily via its derivative the contribution of the inflaton into the F-term SUGRA potential, placing S at the origin—see Section 3.1. It plays also a key role in the resolution of the μ problem of MSSM via the second term in the right-hand side (rhs) of Equation (3b)—see Section 4.2. The inflaton is contained in the system $\bar{\Phi} - \Phi$. We are obliged to restrict ourselves to subplanckian values of $\bar{\Phi}\Phi$ since the imposed symmetries do not forbid non-renormalizable terms of the form $(\bar{\Phi}\Phi)^p$ with $p > 1$—see Section 3.3. The third term in the rhs of Equation (3b) provides the Majorana masses for the N_i^c's—cf. References [12,13,54,55]—and assures the decay [74] of the inflaton to $\widetilde{N}_i^c$, whose subsequent

decay can activate nTL. Here, we work in the so-called N_i^c*-basis*, where M_{iN^c} is diagonal, real and positive. These masses, together with the Dirac neutrino masses in Equation (3a), lead to the light neutrino masses via the seesaw mechanism.

2.2. Kähler Potential

HI is feasible if $W_{\rm HI}$ cooperates with *one* of the following Kähler potentials—cf. Reference [26]:

$$K_1 = -N\ln\left(1+c_+F_+ + F_{1X}(|X|^2)\right) + c_-F_-, \tag{4a}$$

$$K_2 = -N\ln\left(1+c_+F_+\right) + c_-F_- + F_{2X}(|X|^2), \tag{4b}$$

$$K_3 = -N\ln\left(1+c_+F_+\right) + F_{3X}(F_-,|X|^2), \tag{4c}$$

where $N>0$, $X^\gamma = S, H_u, H_d, \widetilde{N}_i^c$ and the complex scalar components of the superfields $\Phi, \bar{\Phi}, S, H_u$ and H_d are denoted by the same symbol whereas this of N_i^c by $\widetilde{N}_i^c$. The functions $F_\pm = |\Phi \pm \bar{\Phi}^*|^2$ assist us in the introduction of shift symmetry for the Higgs fields—cf. Reference [47,48]. In all K's, F_+ is included in the argument of a logarithm with coefficient $-N$ whereas F_- is outside it. As regards the non-inflaton fields X^γ, we assume that they have identical kinetic terms expressed by the functions F_{lX} with $l=1,2,3$. In Table 2 we expose two possible forms for each F_{iX} following Reference [49–51]. These are selected so as to successfully stabilize the scalars X^γ at the origin employing only quadratic terms. Recall [49–51,75–78] that the simplest term $|X|^2$ leads to instabilities for $K=K_1$ and light excitations of X^γ for $K=K_2$ and K_3. The heaviness of these modes is required so that the observed curvature perturbation is generated wholly by our inflaton in accordance with the lack of any observational hint [56] for large non-Gaussianity in the cosmic microwave background.

Table 2. Functional forms of F_{lX} with $l=1,2,3$ shown in the definition of K_1, K_2 and K_3 in Equations (4a)–(4c) respectively.

F_{lX}	Exponential Form	Logarithmic Form
F_{1X}	$\exp\left(-\lvert X\rvert^2/N\right)-1$	$-\ln(1+\lvert X\rvert^2/N)$
F_{2X}	$-N_X\left(\exp\left(-\lvert X\rvert^2/N_X\right)-1\right)$	$N_X\ln(1+\lvert X\rvert^2/N_X)$
F_{3X}	$-N_X\left(\exp\left(-c_-F_-/N_X-\lvert X\rvert^2/N_X\right)-1\right)$	$N_X\ln(1+c_-F_-/N_X+\lvert X\rvert^2/N_X)$

As we show in Section 3.1, the positivity of the kinetic energy of the inflaton sector requires $c_+ < c_-$ and $N>0$. For $r_\pm = c_+/c_- \ll 1$, our models are completely natural in the 't Hooft sense because, in the limits $c_+ \to 0$ and $\lambda \to 0$, they enjoy the following enhanced symmetries

$$\Phi \to \Phi + c, \quad \bar{\Phi} \to \bar{\Phi} + c^* \quad \text{and} \quad X^\gamma \to e^{i\varphi_\gamma}X^\gamma, \tag{5}$$

where c and φ_γ are complex and real numbers respectively and no summation is applied over γ. This enhanced symmetry has a string theoretical origin as shown in Reference [79,80]. In this framework, mainly integer N's are considered which can be reconciled with the observational data. Namely, acceptable inflationary solutions are attained for $N=3$ [$N=2$] if $K=K_1$ [$K=K_2$ or K_3]—see Section 3.4. However, deviation of the N's from these integer values is perfectly acceptable [26,48,81–85] and can have a pronounced impact on the inflationary predictions allowing for a covering of the whole $n_{\rm s}-r$ plane with quite natural values of the relevant parameters.

3. Inflationary Scenario

The salient features of our inflationary scenario are studied at tree level in Section 3.1 and at one-loop level in Section 3.2. We then present its predictions in Section 3.4, calculating a number of observable quantities introduced in Section 3.3.

3.1. Inflationary Potential

Within SUGRA the Einstein frame (EF) action for the scalar fields $z^\alpha = S, \Phi, \bar{\Phi}, H_u, H_d$ and $\widetilde{N}_i^c$ can be written as

$$\mathsf{S} = \int d^4x\sqrt{-\widehat{\mathfrak{g}}}\left(-\frac{1}{2}\widehat{\mathcal{R}} + K_{\alpha\bar{\beta}}\widehat{g}^{\mu\nu}D_\mu z^\alpha D_\nu z^{*\bar{\beta}} - \widehat{V}\right), \tag{6a}$$

where $\widehat{\mathcal{R}}$ is the Ricci scalar and $\mathfrak{g}$ is the determinant of the background Friedmann-Robertson-Walker metric, $g^{\mu\nu}$ with signature $(+,-,-,-)$. We adopt also the following notation

$$K_{\alpha\bar{\beta}} = K_{,z^\alpha z^{*\bar{\beta}}} > 0 \;\text{ and }\; D_\mu z^\alpha = \partial_\mu z^\alpha + igA_\mu^{\mathrm{a}}T^{\mathrm{a}}_{\alpha\beta}z^\beta, \tag{6b}$$

are the covariant derivatives for the scalar fields z^α. Also, g is the unified gauge coupling constant, A_μ^{a} are the vector gauge fields and T^{a} are the generators of the gauge transformations of z^α. Also $\widehat{V}$ is the EF SUGRA scalar potential which can be found via the formula

$$\widehat{V} = \widehat{V}_{\mathrm{F}} + \widehat{V}_{\mathrm{D}} \;\text{ with }\; \widehat{V}_{\mathrm{F}} = e^K\left(K^{\alpha\bar{\beta}}D_\alpha W_{\mathrm{HI}}D^*_{\bar{\beta}}W^*_{\mathrm{HI}} - 3|W_{\mathrm{HI}}|^2\right) \;\text{ and }\; \widehat{V}_{\mathrm{D}} = \frac{1}{2}g^2\sum_{\mathrm{a}}\mathrm{D_a}\mathrm{D_a}, \tag{6c}$$

where we use the notation

$$K^{\alpha\bar{\beta}}K_{\alpha\bar{\gamma}} = \delta^{\bar{\beta}}_{\bar{\gamma}},\; D_\alpha W_{\mathrm{HI}} = W_{\mathrm{HI},z^\alpha} + K_\alpha W_{\mathrm{HI}} \;\text{ and }\; \mathrm{D_a} = z^\alpha\,(T_{\mathrm{a}})^\beta_\alpha\,K_\beta \;\text{ with }\; K_\alpha = K_{,z^\alpha}. \tag{6d}$$

If we express $\Phi, \bar{\Phi}$ and $X^\gamma = S, H_u, H_d, \widetilde{N}_i^c$ according to the parametrization

$$\Phi = \frac{\phi e^{i\theta}}{\sqrt{2}}\cos\theta_\Phi,\;\; \bar{\Phi} = \frac{\phi e^{i\bar{\theta}}}{\sqrt{2}}\sin\theta_\Phi \;\text{ and }\; X^\gamma = \frac{x^\gamma + i\bar{x}^\gamma}{\sqrt{2}}, \tag{7}$$

where $0 \leq \theta_\Phi \leq \pi/2$, we can easily deduce from Equation (6c) that a D-flat direction occurs at

$$x^\gamma = \bar{x}^\gamma = \theta = \bar{\theta} = 0 \;\text{ and }\; \theta_\Phi = \pi/4, \tag{8}$$

along which the only surviving term in Equation (6c) can be written universally as

$$\widehat{V}_{\mathrm{HI}} = e^K K^{SS^*}\,|W_{\mathrm{HI},S}|^2 = \frac{\lambda^2(\phi^2 - M^2)^2}{16 f_{\mathcal{R}}^{2(1+n)}} \;\text{ where }\; f_{\mathcal{R}} = 1 + c_+\phi^2, \tag{9}$$

plays the role of a non-minimal coupling to Ricci scalar in the Jordan frame (JF)—see References [48,75–78]. Also, we set

$$n = \begin{cases}(N-3)/2\\ N/2-1\end{cases} \;\text{ and }\; K^{SS^*} = \begin{cases} f_{\mathcal{R}} \\ 1\end{cases} \;\text{ for }\; \begin{cases} K = K_1\,,\\ K = K_2 \;\text{ and }\; K_3\,.\end{cases} \tag{10}$$

The introduction of n allows us to obtain a unique inflationary potential for all the K's in Equations (4a)–(4c). For $K = K_1$ and $N = 3$ or $K = K_2$ or K_3 and $N = 2$ we get $n = 0$ and $\widehat{V}_{\mathrm{HI}}$ develops an inflationary plateau as in the original case of non-minimal inflation [4,5]. Contrary to that case, though, here we have also c_- which dominates the canonical normalization of ϕ—see Section 3.2—and allows for distinctively different inflationary outputs as shown in References [25,27,28]. Finally, the variation of n above and below zero allows for more drastic deviations [26,48] from the predictions of the original model [4,5]. In particular, for $n < 0$, $\widehat{V}_{\mathrm{HI}}$ remains increasing function of ϕ, whereas for $n > 0$, $\widehat{V}_{\mathrm{HI}}$ develops a local maximum

$$\widehat{V}_{\mathrm{HI}}(\phi_{\max}) = \frac{\lambda^2 n^{2n}}{16c_+^2(1+n)^{2(1+n)}} \;\text{ at }\; \phi_{\max} = \frac{1}{\sqrt{c_+ n}}\,. \tag{11}$$

In a such case we are forced to assume that hilltop [86] HI occurs with ϕ rolling from the region of the maximum down to smaller values. Therefore, a mild tuning of the initial conditions is required which can be quantified somehow defining [87–90] the quantity

$$\Delta_{\max\star} = \left(\phi_{\max} - \phi_\star\right)/\phi_{\max}\,, \tag{12}$$

$\phi_\star$ is the value of ϕ when the pivot scale $k_\star = 0.05/\text{Mpc}$ crosses outside the inflationary horizon. The naturalness of the attainment of HI increases with $\Delta_{\max\star}$ and it is maximized when $\phi_{\max} \gg \phi_\star$ which result to $\Delta_{\max\star} \simeq 1$.

The structure of $\widehat{V}_{\rm HI}$ as a function of ϕ is displayed in Figure 1. We take $\phi_\star = 1$, $r_\pm = 0.03$ and $n = -0.1$ (light gray line), $n = 0$ (black line) and $n = 0.1$ (gray line). Imposing the inflationary requirements mentioned in Section 3.4 we find the corresponding values of λ and c_- which are $(7.75, 6.64 \text{ or } 5.3)\times 10^{-3}$ and $(1.7,\ 1.46 \text{ or } 1.24)\times 10^{2}$ respectively. The corresponding observable quantities are found numerically to be $n_{\rm s} = 0.971, 0.969$ or 0.966 and $r = 0.045, 0.03$ or 0.018 with $a_{\rm s} \simeq -5\times 10^{-4}$ in all cases. We see that $\widehat{V}_{\rm HI}$ is a monotonically increasing function of ϕ for $n \leq 0$ whereas it develops a maximum at $\phi_{\max} = 1.64$, for $n = 0.1$, which leads to a mild tuning of the initial conditions of HI since $\Delta_{\max\star} = 39\%$, according to the criterion introduced above. It is also remarkable that r increases with the inflationary scale, $\widehat{V}_{\rm HI}^{1/4}$, which, in all cases, approaches the SUSY GUT scale $M_{\rm GUT} \simeq 8.2\times 10^{-3}$ facilitating the interpretation of the inflaton as a GUT-scale Higgs field.

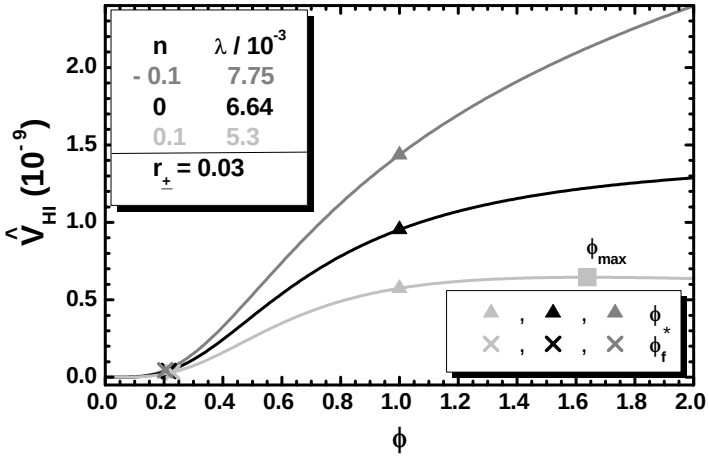

Figure 1. The inflationary potential $\widehat{V}_{\rm HI}$ as a function of ϕ for $\phi > 0$, and $r_\pm \simeq 0.03$, and $n = -0.1$, $\lambda = 7.75\times 10^{-3}$ (gray line), $n = 0$, $\lambda = 6.64\times 10^{-3}$ (black line), or $n = +0.1$, $\lambda = 5.3\times 10^{-3}$ (light gray line). The values of $\phi_\star$, $\phi_{\rm f}$ and $\phi_{\max}$ (for $n = 1/10$) are also indicated.

3.2. Stability and One-Loop Radiative Corrections

As deduced from Equation (9) $\widehat{V}_{\rm HI}$ is independent from c_- which dominates, though, the canonical normalization of the inflaton. To specify it together with the normalization of the other fields, we note that, for all K's in Equations (4a)–(4c), $K_{\alpha\bar\beta}$ along the configuration in Equation (8) takes the form

$$\left(K_{\alpha\bar\beta}\right) = \text{diag}\left(M_\pm, \underbrace{K_{\gamma\bar\gamma}, ..., K_{\gamma\bar\gamma}}_{\text{8 elements}}\right), \tag{13a}$$

with

$$M_K = \frac{1}{f_{\mathcal{R}}^2}\begin{pmatrix}\kappa & \bar\kappa\\ \bar\kappa & \kappa\end{pmatrix} \text{ and } K_{\gamma\bar\gamma} = \begin{cases} 1/f_{\mathcal{R}} \\ 1\end{cases} \text{ for } \begin{cases} K = K_1\,, \\ K = K_2 \text{ and } K_3\,. \end{cases} \tag{13b}$$

Here $\kappa = c_- f_{\mathcal{R}}^2 - N c_+$ and $\bar{\kappa} = N c_+^2 \phi^2$. Upon diagonalization of $M_\pm$ we find its eigenvalues which are

$$\kappa_+ = c_- \left(1 + N r_\pm (c_+ \phi^2 - 1)/f_{\mathcal{R}}^2\right) \simeq c_- \;\text{ and }\; \kappa_- = c_- \left(1 - N r_\pm / f_{\mathcal{R}}\right), \tag{14}$$

where the positivity of κ_- is assured during and after HI for

$$r_\pm < f_{\mathcal{R}}/N \;\text{ with }\; r_\pm = c_+/c_- . \tag{15}$$

Given that $f_{\mathcal{R}} > 1$ and $\langle f_{\mathcal{R}} \rangle \simeq 1$, Equation (15) implies that the maximal possible $r_\pm$ is $r_\pm^{\max} \simeq 1/N$. Given that N tends to 3 [2] for $K = K_1$ [$K = K_2$ or K_3], the inequality above discriminates somehow the allowed parameter space for the various choices of K's in Equations (4a) and (4b).

Inserting Equations (7) and (13b) in the second term of the rhs of Equation (6a) we can, then, specify the EF canonically normalized fields, which are denoted by hat, as follows:

$$\begin{aligned} K_{\alpha\bar{\beta}} \dot{z}^\alpha \dot{z}^{*\bar{\beta}} &= \frac{\kappa_+}{2}\left(\dot{\phi}^2 + \frac{1}{2}\phi^2 \dot{\theta}_+^2\right) + \frac{\kappa_-}{2}\phi^2\left(\frac{1}{2}\dot{\theta}_-^2 + \dot{\theta}_\Phi^2\right) + \frac{1}{2}K_{\gamma\bar{\gamma}}\left(\dot{x}^{\gamma 2} + \dot{\bar{x}}^{\gamma 2}\right) \\ &\simeq \frac{1}{2}\left(\dot{\hat{\phi}}^2 + \dot{\hat{\theta}}_+^2 + \dot{\hat{\theta}}_-^2 + \dot{\hat{\theta}}_\Phi^2 + \dot{\hat{x}}^{\gamma 2} + \dot{\hat{\bar{x}}}^{\gamma 2}\right), \end{aligned} \tag{16a}$$

where $\theta_\pm = \left(\bar{\theta} \pm \theta\right)/\sqrt{2}$ and the dot denotes derivation the cosmic time t. The hatted fields of the $\Phi - \bar{\Phi}$ system can be expressed in terms of the initial (unhatted) ones via the relations

$$\frac{d\widehat{\phi}}{d\phi} = J = \sqrt{\kappa_+},\; \widehat{\theta}_+ = \frac{J}{\sqrt{2}}\phi\theta_+,\; \widehat{\theta}_- = \sqrt{\frac{\kappa_-}{2}}\phi\theta_-,\; \text{and}\; \widehat{\theta}_\Phi = \sqrt{\kappa_-}\phi\left(\theta_\Phi - \frac{\pi}{4}\right). \tag{16b}$$

As regards the non-inflaton fields, the (approximate) normalization is implemented as follows

$$(\widehat{x}^\gamma, \widehat{\bar{x}}^\gamma) = \sqrt{K_{\gamma\bar{\gamma}}}(x^\gamma, \bar{x}^\gamma). \tag{16c}$$

As we show below, the masses of the scalars besides $\widehat{\phi}$ during HI are heavy enough such that the dependence of the hatted fields on ϕ does not influence their dynamics—see also Reference [12,13].

We can verify that the inflationary direction in Equation (8) is stable wrt the fluctuations of the non-inflaton fields. To this end, we construct the mass-squared spectrum of the scalars taking into account the canonical normalization of the various fields in Equation (16a)—for details see Reference [48]. In the limit $c_- \gg c_+$, we find the expressions of the masses squared $\widehat{m}_{z^\alpha}^2$ (with $z^\alpha = \theta_+, \theta_\Phi, x^\gamma$ and $\bar{x}^\gamma$) arranged in Table 3. These results approach rather well the quite lengthy, exact expressions taken into account in our numerical computation. The various unspecified there eigenvalues are defined as follows:

$$h_\pm = (h_u \pm h_d)/\sqrt{2},\;\; \bar{h}_\pm = (\bar{h}_u \pm \bar{h}_d)/\sqrt{2} \;\text{ and }\; \widehat{\psi}_\pm = (\widehat{\psi}_{\Phi+} \pm \widehat{\psi}_S)/\sqrt{2}, \tag{17a}$$

where the (unhatted) spinors ψ_Φ and $\psi_{\bar{\Phi}}$ associated with the superfields Φ and $\bar{\Phi}$ are related to the normalized (hatted) ones in Table 3 as follows:

$$\widehat{\psi}_{\Phi\pm} = \sqrt{\kappa_\pm}\psi_{\Phi\pm} \;\text{ with }\; \psi_{\Phi\pm} = (\psi_\Phi \pm \psi_{\bar{\Phi}})/\sqrt{2}. \tag{17b}$$

From Table 3 it is evident that $0 < N_X \leq 6$ assists us to achieve $m_s^2 > \widehat{H}_{\rm HI}^2 = \widehat{V}_{\rm HI}/3$—in accordance with the results of Reference [49–51]—and also enhances the ratios $m_{X^{\bar{\gamma}}}^2/\widehat{H}_{\rm HI}^2$ for $X^{\bar{\gamma}} = H_u, H_d, \widetilde{N}_i^c$ wrt the values that we would have obtained, if we had used just canonical terms in the K's. On the other hand, $\widehat{m}_{h-}^2 > 0$ requires

$$\lambda_\mu < \lambda(1 + c_+\phi^2/N)/4\left(1/\phi^2 + c_+\right) \qquad \text{for } K = K_1; \tag{18a}$$

$$\lambda_\mu < \lambda\phi^2(1 + 1/N_X)/4 \qquad \text{for } K = K_2 \text{ and } K_3. \tag{18b}$$

In both cases, the quantity in the rhs of the inequality takes its minimal value at $\phi = \phi_{\rm f}$ and numerically equals to $2 \times 10^{-5} - 10^{-6}$. Similar numbers are obtained in Reference [54] although that higher order terms in the Kähler potential are invoked there. We do not consider such a condition on λ_μ as unnatural, given that h_{1U} in Equation (3a) is of the same order of magnitude too—cf. Reference [91]. Note that the due hierarchy in Equations (18a) and (18b) between λ_μ and λ differs from that imposed in the models [73] of F-term hybrid inflation, where S plays the role of inflaton and $\Phi, \bar{\Phi}$, H_u and H_d are confined at zero. Indeed, in that case we demand [73] $\lambda_\mu > \lambda$ so that the tachyonic instability in the $\Phi - \bar{\Phi}$ direction occurs first, and the $\Phi - \bar{\Phi}$ system start evolving towards its v.e.v, whereas H_u and H_d continue to be confined to zero. In our case, though, the inflaton is included in the $\bar{\Phi} - \Phi$ system while S and the $H_u - H_d$ system are safely stabilized at the origin both during and after HI. Therefore, ϕ is led at its vacuum whereas S, H_u and H_d take their non-vanishing electroweak scale v.e.vs afterwards.

In Table 3 we display also the mass M_{BL} of the gauge boson which becomes massive having 'eaten' the Goldstone boson θ_-. This signals the fact that G_{B-L} is broken during HI. Shown are also the masses of the corresponding fermions—note that the fermions $\tilde{h}_\pm$ and $\tilde{\bar{h}}_\pm$, associated with $h_\pm$ and $\bar{h}_\pm$ remain massless. The derived mass spectrum can be employed in order to find the one-loop radiative corrections, $\Delta\widehat{V}_{\rm HI}$ to $\widehat{V}_{\rm HI}$. Considering SUGRA as an effective theory with cutoff scale equal to $m_{\rm P}$, the well-known Coleman-Weinberg formula [92] can be employed self-consistently taking into account the masses which lie well below $m_{\rm P}$, i.e., all the masses arranged in Table 3 besides M_{BL} and $\widehat{m}_{\theta_\Phi}$. Therefore, the one-loop correction to $\widehat{V}_{\rm HI}$ reads

$$\begin{aligned}\Delta\widehat{V}_{\rm HI} &= \frac{1}{64\pi^2}\left(\widehat{m}^4_{\theta+}\ln\frac{\widehat{m}^2_{\theta+}}{\Lambda^2} + 2m_s^4\ln\frac{m_s^2}{\Lambda^2} + 4m^4_{h+}\ln\frac{m^2_{h+}}{\Lambda^2} + 4m^4_{h-}\ln\frac{m^2_{h-}}{\Lambda^2}\right.\\ &+ \left. 2\sum_{i=1}^{3}\left(m^4_{i\tilde{\nu}^c}\ln\frac{m^2_{i\tilde{\nu}^c}}{\Lambda^2} - m^4_{iN^c}\ln\frac{m^2_{iN^c}}{\Lambda^2}\right) - 4\widehat{m}^4_{\psi_\pm}\ln\frac{\widehat{m}^2_{\psi_\pm}}{\Lambda^2}\right),\end{aligned} \tag{19}$$

where Λ is a renormalization group(RG) mass scale. The resulting $\Delta\widehat{V}_{\rm HI}$ lets intact our inflationary outputs, provided that Λ is determined by requiring $\Delta\widehat{V}_{\rm HI}(\phi_\star) = 0$ or $\Delta\widehat{V}_{\rm HI}(\phi_{\rm f}) = 0$. These conditions yield $\Lambda \simeq 3.2 \times 10^{-5} - 1.4 \times 10^{-4}$ and render our results practically independent of Λ since these can be derived exclusively by using $\widehat{V}_{\rm HI}$ in Equation (9) with the various quantities evaluated at Λ—cf. Reference [48]. Note that their renormalization-group running is expected to be negligible because Λ is close to the inflationary scale $\widehat{V}^{1/4}_{\rm HI} \simeq (3-7) \times 10^{-3}$—see Figure 1.

Table 3. The mass squared spectrum of our models along the inflationary trajectory in Equation (8) for $K = K_1, K_2, K_3$ and $\phi \ll 1$. To avoid very lengthy formulas, we neglect terms proportional to $M \ll \phi$.

Fields	**Eigenstates**	**Masses Squared**			
			$K = K_1$	$K = K_2$	$K = K_3$
14 Real	$\widehat{\theta}_+$	$\widehat{m}^2_{\theta+}$	$6\widehat{H}^2_{\rm HI}$		$6(1+1/N_X)\widehat{H}^2_{\rm HI}$
Scalars	$\widehat{\theta}_\Phi$	$\widehat{m}^2_{\theta_\Phi}$	$M^2_{BL} + 6\widehat{H}^2_{\rm HI}$		$M^2_{BL} + 6(1+1/N_X)\widehat{H}^2_{\rm HI}$
	$s, \bar{s}$	m^2_s	$6c_+\phi^2\widehat{H}^2_{\rm HI}/N$		$6\widehat{H}^2_{\rm HI}/N_X$
	$h_\pm, \bar{h}_\pm$	$m^2_{h\pm}$	$3\widehat{H}^2_{\rm HI}\left(1 + c_+\phi^2/N \pm 4\lambda_\mu(1/\phi^2 + c_+)/\lambda\right)$		$3\widehat{H}^2_{\rm HI}\left(1 + 1/N_X \pm 4\lambda_\mu/\lambda\phi^2\right)$
	$\tilde{\nu}^c_i, \tilde{\bar{\nu}}^c_i$	$m^2_{i\tilde{\nu}^c}$	$3\widehat{H}^2_{\rm HI}\left(1 + c_+\phi^2/N + 16\lambda^2_{iN^c}(1/\phi^2 + c_+)/\lambda^2\right)$		$3\widehat{H}^2_{\rm HI}\left(1 + 1/N_X + 16\lambda^2_{iN^c}/\lambda^2\phi^2\right)$
1 Gauge Boson	A_{BL}	M^2_{BL}	$g^2c_-\left(1 - Nr_\pm/f_{\mathcal{R}}\right)\phi^2$		
7 Weyl	$\widehat{\psi}_\pm$	$\widehat{m}^2_{\psi\pm}$	$6\left((N-3)c_+\phi^2 - 2\right)^2\widehat{H}^2_{\rm HI}/c_-\phi^2 f^2_{\mathcal{R}}$		$6\left((N-2)c_+\phi^2 - 2\right)^2\widehat{H}^2_{\rm HI}/c_-\phi^2 f^2_{\mathcal{R}}$
Spinors	N^c_i	$m^2_{iN^c}$	$48\lambda^2_{iN^c}\widehat{H}^2_{\rm HI}/\lambda^2\phi^2$		
	$\lambda_{BL}, \widehat{\psi}_{\Phi-}$	M^2_{BL}	$g^2c_-\left(1 - Nr_\pm/f_{\mathcal{R}}\right)\phi^2$		

3.3. Inflationary Observables

A period of slow-roll HI is determined by the condition—see e.g., Reference [93–95]

$$\max\{\widehat{\epsilon}(\phi), |\widehat{\eta}(\phi)|\} \leq 1, \tag{20}$$

where

$$\widehat{\epsilon} = \frac{1}{2}\left(\frac{\widehat{V}_{\rm HI,\widehat{\phi}}}{\widehat{V}_{\rm HI}}\right)^2 = \frac{1}{2J^2}\left(\frac{\widehat{V}_{\rm HI,\phi}}{\widehat{V}_{\rm HI}}\right)^2 \simeq \frac{8(1-nc_+\phi^2)^2}{c_-\phi^2 f_{\mathcal{R}}^2}, \tag{21a}$$

and

$$\widehat{\eta} = \frac{\widehat{V}_{\rm HI,\widehat{\phi}\widehat{\phi}}}{\widehat{V}_{\rm HI}} = \frac{1}{J^2}\left(\frac{\widehat{V}_{\rm HI,\phi\phi}}{\widehat{V}_{\rm HI}} - \frac{\widehat{V}_{\rm HI,\phi}}{\widehat{V}_{\rm HI}}\frac{J_{,\phi}}{J}\right) = 4\,\frac{3-3(1+3n)c_+\phi^2 + n(1+4n)c_+^2\phi^4}{c_-\phi^2 f_{\mathcal{R}}^2}\,. \tag{21b}$$

Expanding $\widehat{\epsilon}$ and $\widehat{\eta}$ for $\phi \ll 1$ we can find from Equation (20) that HI terminates for $\phi = \phi_{\rm f}$ such that

$$\phi_{\rm f} \simeq \max\left\{\frac{2\sqrt{2/c_-}}{\sqrt{1+16(1+n)r_\pm}}, \frac{2\sqrt{3/c_-}}{\sqrt{1+36(1+n)r_\pm}}\right\}. \tag{22}$$

The number of e-foldings, $\widehat{N}_\star$, that the pivot scale $k_\star = 0.05/\text{Mpc}$ suffers during HI can be calculated through the relation

$$\widehat{N}_\star = \int_{\widehat{\phi}_{\rm f}}^{\widehat{\phi}_\star} d\widehat{\phi}\,\frac{\widehat{V}_{\rm HI}}{\widehat{V}_{\rm HI,\widehat{\phi}}} \simeq \begin{cases} ((1+c_+\phi_\star^2)^2-1)/16r_\pm & \text{for } n=0\,, \\ -\left(nc_+\phi_\star^2 + (1+n)\ln(1-nc_+\phi_\star^2)\right)/8n^2r_\pm & \text{for } n\neq 0\,, \end{cases} \tag{23}$$

where $\widehat{\phi}_\star$ is the value of $\widehat{\phi}$ when $k_\star$ crosses the inflationary horizon. As regards the consistency of the relation above for $n > 0$, we note that we get $nc_+\phi_\star^2 < 1$ in all relevant cases and so, $\ln(1-nc_+\phi_\star^2) < 0$ assures the positivity of $\widehat{N}_\star$. Given that $\phi_{\rm f} \ll \phi_\star$, we can write $\phi_\star$ as a function of $\widehat{N}_\star$ as follows:

$$\phi_\star \simeq \sqrt{\frac{f_{n\star}-1}{c_+}} \text{ with } f_{n\star} = \begin{cases} \left(1+16r_\pm\widehat{N}_\star\right)^{1/2} & \text{for } n=0\,, \\ (1+n)/n\,(1+W_k\,(y/(1+n))) & \text{for } n\neq 0\,. \end{cases} \tag{24}$$

Here W_k is the Lambert W or product logarithmic function [96] and the parameter y is defined as $y = -\exp\left(-(1+8n^2\widehat{N}_\star r_\pm)/(1+n)\right)$. We take $k=0$ for $n \geq 0$ and $k=-1$ for $n<0$. We can impose a lower bound on c_- above which $\phi_\star \leq 1$ for every $r_\pm$. Indeed, from Equation (24) we have

$$\phi_\star \leq 1 \;\Rightarrow\; c_- \geq (f_{n\star}-1)/r_\pm, \tag{25}$$

and so, our proposal can be stabilized against corrections from higher order terms of the form $(\Phi\bar{\Phi})^p$ with $p > 1$ in $W_{\rm HI}$—see Equation (3b). Despite the fact that c_- may take relatively large values, the corresponding effective theory is valid up to $m_{\rm P} = 1$—contrary to the pure quartic nMI [36–38]. To clarify further this point we have to identify the ultraviolet cut-off scale $\Lambda_{\rm UV}$ of theory analyzing the small-field behavior of our models. More specifically, we expand about $\langle\phi\rangle = M \ll 1$ the second term in the rhs of Equation (6a) for $\mu = \nu = 0$ and $\widehat{V}_{\rm HI}$ in Equation (9). Our results can be written in terms of $\widehat{\phi}$ as

$$J^2\dot{\phi}^2 \simeq \left(1+3Nr_\pm^2\widehat{\phi}^2 - 5Nr_\pm^3\widehat{\phi}^4 + \cdots\right)\dot{\widehat{\phi}}^2; \tag{26a}$$

$$\widehat{V}_{\rm HI} \simeq \frac{\lambda^2\widehat{\phi}^4}{16c_-^2}\left(1-2(1+n)r_\pm\widehat{\phi}^2 + (3+5n)r_\pm^2\widehat{\phi}^4 - \cdots\right). \tag{26b}$$

From the expressions above we conclude that $\Lambda_{\rm UV} = m_{\rm P}$ since $r_\pm \leq 1$ due to Equation (15). Although the expansions presented below, are valid only during reheating we consider the extracted $\Lambda_{\rm UV}$ as the overall cut-off scale of the theory since the reheating is regarded [38] as an unavoidable stage of HI.

The power spectrum $A_{\rm s}$ of the curvature perturbations generated by ϕ at the pivot scale $k_\star$ is estimated as follows:

$$\sqrt{A_{\rm s}} = \frac{1}{2\sqrt{3}\,\pi}\,\frac{\widehat{V}_{\rm HI}(\widehat{\phi}_\star)^{3/2}}{|\widehat{V}_{{\rm HI},\widehat{\phi}}(\widehat{\phi}_\star)|} \simeq \frac{\lambda\sqrt{c_-}}{32\sqrt{3}\pi}\,\frac{\phi_\star^3 f_{\mathcal{R}}(\phi_\star)^{-n}}{1-nc_+\phi_\star^2}\,. \tag{27}$$

The resulting relation reveals that λ is proportional to c_- for fixed n and $r_\pm$. Indeed, plugging Equation (24) into the expression above, we find

$$\lambda = 32\sqrt{3A_{\rm s}}\pi c_- r_\pm^{3/2} f_{n\star}^n\,\frac{n(1-f_{n\star})+1}{(f_{n\star}-1)^{3/2}}\,. \tag{28}$$

At the same pivot scale, we can also calculate $n_{\rm s}$, its running, $a_{\rm s}$, and r via the relations

$$n_{\rm s} = 1 - 6\widehat{\epsilon}_\star + 2\widehat{\eta}_\star \simeq 1 - 4n^2 r_\pm - 2n\frac{r_\pm^{1/2}}{\widehat{N}_\star^{1/2}} - \frac{3-2n}{2\widehat{N}_\star} - \frac{3-n}{8(\widehat{N}_\star^3 r_\pm)^{1/2}}\,, \tag{29a}$$

$$a_{\rm s} = \frac{2}{3}\left(4\widehat{\eta}_\star^2 - (n_{\rm s}-1)^2\right) - 2\widehat{\xi}_\star \simeq -\frac{n r_\pm^{1/2}}{\widehat{N}_\star^{3/2}} - \frac{3-2n}{2\widehat{N}_\star^2}, \tag{29b}$$

$$r = 16\widehat{\epsilon}_\star \simeq -\frac{8n}{\widehat{N}_\star} + \frac{3+2n}{6\widehat{N}_\star^2 r_\pm} + \frac{6-n}{3(\widehat{N}_\star^3 r_\pm)^{1/2}} + \frac{8n^2 r_\pm^{1/2}}{\widehat{N}_\star^{1/2}}\,, \tag{29c}$$

where $\widehat{\xi} = \widehat{V}_{{\rm HI},\widehat{\phi}}\widehat{V}_{{\rm HI},\widehat{\phi}\widehat{\phi}\widehat{\phi}}/\widehat{V}_{\rm HI}^2$ and the variables with subscript $\star$ are evaluated at $\phi = \phi_\star$.

3.4. Comparison with Observations

The approximate analytic expressions above can be verified by the numerical analysis of our model. Namely, we apply the accurate expressions in Equations (23) and (27) and confront the corresponding observables with the requirements [56]

$$\widehat{N}_\star \simeq 61.5 + \ln\frac{\widehat{V}_{\rm HI}(\phi_\star)^{1/2}}{\widehat{V}_{\rm HI}(\phi_{\rm f})^{1/4}} + \frac{1}{2}f_{\mathcal{R}}(\phi_\star) \tag{30a}$$

$$\text{and } A_{\rm s}^{1/2} \simeq 4.627\times 10^{-5}\,. \tag{30b}$$

We, thus, restrict λ and $\phi_\star$ and compute the model predictions via Equations (29a)–(29c) for any selected n and $r_\pm$. In Equation (30a) we consider an equation-of-state parameter $w_{\rm int} = 1/3$ corresponding to quartic potential which is expected to approximate rather well $\widehat{V}_{\rm HI}$ for $\phi \ll 1$. For rigorous comparison with observations we compute $r_{0.002} = 16\widehat{\epsilon}(\widehat{\phi}_{0.002})$ where $\widehat{\phi}_{0.002}$ is the value of $\widehat{\phi}$ when the scale $k = 0.002/{\rm Mpc}$, which undergoes $\widehat{N}_{0.002} = \widehat{N}_\star + 3.22$ e-foldings during HI, crosses the horizon of HI. These must be in agreement with the fitting of the *Planck*, Baryon Acoustic Oscillations (BAO) and BICEP2/*Keck Array* data [34,35] with ΛCDM+r model, i.e.,

$$n_{\rm s} = 0.968 \pm 0.009 \tag{31a}$$

$$\text{and } r \leq 0.07, \tag{31b}$$

at 95% confidence level (c.l.) with $|a_{\rm s}| \ll 0.01$.

Let us clarify here that the free parameters of our models are n, $r_\pm$ and λ/c_- and not n, c_-, c_+ and λ as naively expected. Indeed, if we perform the rescalings

$$\Phi \to \Phi/\sqrt{c_-}, \;\; \bar{\Phi} \to \bar{\Phi}/\sqrt{c_-} \;\; \text{and} \;\; S \to S, \tag{32}$$

W in Equation (3b) depends on λ/c_-, given that $\phi \gg M$, and the K's in Equations (4a)–(4c) depend on n and $r_\pm$. As a consequence, $\widehat{V}_{\rm HI}$ depends exclusively on λ/c_-, n and $r_\pm$. Since the λ/c_- variation is rather trivial—see Reference [25]—we focus on the variation of the other parameters.

Our results are displayed in Figure 2. Namely, in Figure 2a we show a comparison of the models' predictions against the observational data [34,35] in the $n_{\rm s} - r_{0.002}$ plane. We depict the theoretically allowed values with dot-dashed, double dot-dashed, solid and dashed lines for $n = 0.2, 0.1, 0$ and -0.1 respectively. The variation of $r_\pm$ is shown along each line. For low enough $r_\pm$'s—i.e., $r_\pm \leq 0.0005$—the various lines converge to $(n_{\rm s}, r_{0.002}) \simeq (0.947, 0.28)$ obtained within minimal quartic inflation defined for $c_+ = 0$. Increasing $r_\pm$ the various lines enter the observationally allowed regions, for $r_\pm$ equal to a minimal value $r_\pm^{\rm min}$, and cover them. The lines corresponding to $n = 0, -0.1$ terminate for $r_\pm = r_\pm^{\rm max} \simeq 0.5$, beyond which Equation (15) is violated. Finally, the lines drawn with $n = 0.2$ or $n = 0.1$ cross outside the allowed corridors and so the $r_\pm^{\rm max}$'s, are found at the intersection points. From Figure 2a we infer that the lines with $n > 0$ [$n < 0$] cover the left lower [right upper] corner of the allowed range. As we anticipated in Section 3.1, for $n > 0$ HI is of hilltop type. The relevant parameter $\Delta_{\rm max\star}$ ranges from 0.07 to 0.66 for $n = 0.1$ and from 0.19 to 0.54 for $n = 0.2$ where $\Delta_{\rm max\star}$ increases as $r_\pm$ drops. That is, the required tuning is not severe mainly for $r_\pm < 0.1$.

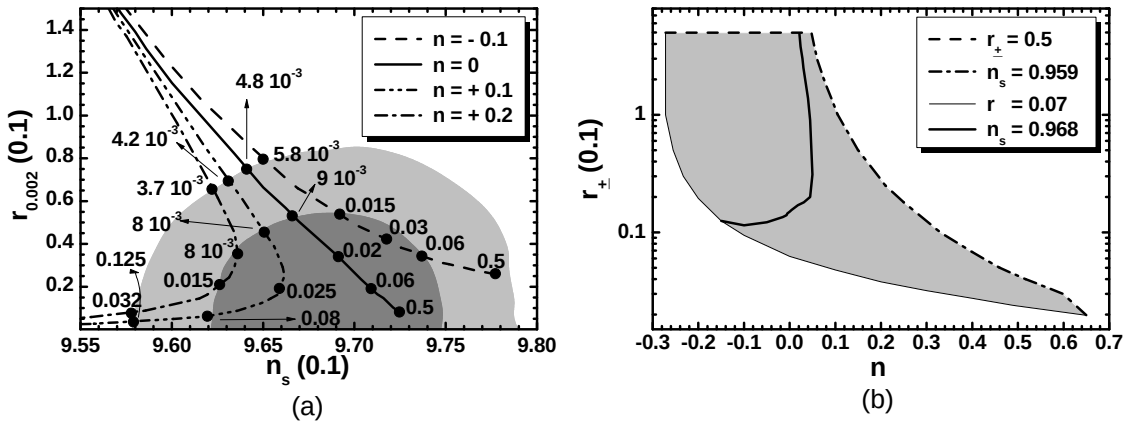

Figure 2. (**a**) Allowed curves in the $n_{\rm s} - r_{0.002}$ plane for $K = K_2$ and K_3, $n = -0.1, 0, 0.1, 0.2$ with the $r_\pm$ values indicated on the curves—the marginalized joint 68% [95%] regions from *Planck*, BAO and BK14 data are depicted by the dark [light] shaded contours; (**b**) Allowed (shaded) regions in the $n - r_\pm$ plane for $K = K_2$ and K_3. The conventions adopted for the various lines are shown.

As deduced from Figure 2a, the observationally favored region can be wholly filled varying conveniently n and $r_\pm$. It would, therefore, interesting to delineate the allowed region of our models in the $n - r_\pm$ plane, as shown in Figure 2b. The conventions adopted for the various lines are also shown in the legend of the plot. In particular, the allowed (shaded) region is bounded by the dashed line, which originates from Equation (15), and the dot-dashed and thin lines along which the lower and upper bounds on $n_{\rm s}$ and r in Equation (31) are saturated respectively. We remark that increasing $r_\pm$ with $n = 0$, r decreases, in accordance with our findings in Figure 2a. On the other hand, $r_\pm$ takes more natural—in the sense of the discussion at the end of Section 2.2—values (lower than unity) for larger values of $|n|$ where hilltop HI is activated. Fixing $n_{\rm s}$ to its central value in Equation (31a) we obtain

the thick solid line along which we get clear predictions for $(n, r_\pm)$ and so, the remaining inflationary observables. Namely, we find

$$-1.21 \lesssim \frac{n}{0.1} \lesssim 0.215, \;\; 0.12 \lesssim \frac{r_\pm}{0.1} \lesssim 5, \;\; 0.4 \lesssim \frac{r}{0.01} \lesssim 7 \;\text{ and }\; 0.25 \lesssim 10^5 \frac{\lambda}{c_-} \lesssim 2.6\,. \tag{33}$$

Hilltop HI is attained for $0 < n \leq 0.0215$ and there, we get $\Delta_{\max\star} \gtrsim 0.4$. The parameter a_s is confined in the range $-(5-6)\times 10^{-4}$ and so, our models are consistent with the fitting of data with the ΛCDM+r model [34]. Moreover, our models are testable by the forthcoming experiments like Bicep3 [97], PRISM [98] and LiteBIRD [99] searching for primordial gravity waves since $r \gtrsim 0.0019$.

Had we employed $K = K_1$, the various lines ended at $r_\pm \simeq 0.5$ in Figure 2a and the allowed region in Figure 2b would have been shortened until $r_\pm \simeq 0.33$. This bound would have yielded slightly larger $r^{\min}_{0.002}$'s. Namely, $r^{\min}_{0.002} \simeq 0.0084$ or 0.026 for $n = 0$ or -0.1 respectively—the $r^{\min}_{0.002}$'s for $n > 0$ are let unaffected. The lower bound of $r/0.01$ and the upper ones on $r_\pm/0.1$ and $10^5\lambda/c_-$ in Equation (33) become 0.64, 3.3 and 2.1 whereas the bounds on a_s remain unaltered.

4. Higgs Inflation and μ Term of MSSM

A byproduct of the R symmetry associated with our model is that it assists us to understand the origin of μ term of MSSM. To see how this works, we first—in Section 4.1—derive the SUSY potential of our models, and then—in Section 4.2—we study the generation of the μ parameter and investigate the possible consequences for the phenomenology of MSSM—see Section 4.3. Here and henceforth we restore units, i.e., we take $m_P = 2.433 \times 10^{18}$ GeV.

4.1. SUSY Potential

Since $\widehat{V}_{\rm HI}$ in Equation (9) is non-renormalizable, its SUSY limit $V_{\rm SUSY}$ depends not only on $W_{\rm HI}$ in Equation (3b), but also on the K's in Equations (4a)–(4c). In particular, $V_{\rm SUSY}$ turns out to be [100]

$$V_{\rm SUSY} = \widetilde{K}^{\alpha\bar{\beta}} W_{{\rm HI}\alpha} W^*_{{\rm HI}\bar{\beta}} + \frac{g^2}{2}\sum_{\rm a} {\rm D_a D_a}\,, \tag{34a}$$

where $\widetilde{K}$ is the limit of the aforementioned K's for $m_P \to \infty$ which is

$$\widetilde{K} = c_- F_- - N c_+ F_+ + |S|^2 + |H_u|^2 + |H_d|^2 + |\widetilde{N}^c_i|^2\,. \tag{34b}$$

Upon substitution of $\widetilde{K}$ into Equation (34a) we obtain

$$V_{\rm SUSY} = \lambda^2 \left|\Phi\Phi - \frac{1}{4}M^2 + \frac{\lambda_\mu}{\lambda} H_u H_d\right|^2 + \frac{1}{c_-(1-N r_\pm)}\left(\left|\lambda S\Phi + \lambda_{iN^c}\widetilde{N}^{c2}\right|^2 + \lambda^2 |S\bar{\Phi}|^2\right) +$$
$$\lambda^2_\mu |S|^2\left(|H_u|^2 + |H_d|^2\right) + 4\lambda^2_{iN^c}|\bar{\Phi}\widetilde{N}^c_i|^2 + \frac{g^2}{2}\left(c_-(1-N r_\pm)\left(|\Phi|^2 - |\bar{\Phi}|^2\right) + |\widetilde{N}^c_i|^2\right)^2. \tag{34c}$$

From the last equation, we find that the SUSY vacuum lies along the D-flat direction $|\bar{\Phi}| = |\Phi|$ with

$$\langle S\rangle = \langle H_u\rangle = \langle H_d\rangle = \langle \widetilde{N}^c_i\rangle = 0 \;\text{ and }\; |\langle\Phi\rangle| = |\langle\bar{\Phi}\rangle| = M/2\,. \tag{35}$$

As a consequence, $\langle\Phi\rangle$ and $\langle\bar{\Phi}\rangle$ break spontaneously $U(1)_{B-L}$ down to $\mathbb{Z}_2^{B-L}$. Since $U(1)_{B-L}$ is already broken during HI, no cosmic string are formed—contrary to what happens in the models of the standard F-term hybrid inflation [6–11,73,87–90], which employ $W_{\rm HI}$ in Equation (3b) too.

4.2. Generation of the μ Term of MSSM

The contributions from the soft SUSY breaking terms, although negligible during HI, since these are much smaller than ϕ, may shift [54,73] slightly $\langle S\rangle$ from zero in Equation (35). Indeed, the relevant potential terms are

$$V_{\rm soft}=\left(\lambda A_\lambda S\bar{\Phi}\Phi+\lambda_\mu A_\mu S H_u H_d+\lambda_{iN^c}A_{iN^c}\Phi\widetilde{N}_i^{c2}-{\rm a}_S S\lambda M^2/4+{\rm h.c.}\right)+m_\gamma^2\left|X^\gamma\right|^2, \tag{36}$$

where m_γ, A_λ, A_μ, A_{iN^c} and a_S are soft SUSY breaking mass parameters. Rotating S in the real axis by an appropriate R-transformation, choosing conveniently the phases of A_λ and a_S so as the total low energy potential $V_{\rm tot}=V_{\rm SUSY}+V_{\rm soft}$ to be minimized—see Equation (34c)—and substituting in $V_{\rm soft}$ the SUSY v.e.vs of $\Phi,\bar{\Phi}$, H_u, H_d and N_i^c from Equation (35) we get

$$\langle V_{\rm tot}(S)\rangle=\lambda^2 M^2S^2/2c_-(1-Nr_\pm)-\lambda{\rm a}_{3/2}m_{3/2}M^2S, \tag{37a}$$

where we take into account that $m_S\ll M$ and we set $|A_\lambda|+|{\rm a}_S|=2{\rm a}_{3/2}m_{3/2}$ with $m_{3/2}$ being the $\widetilde{G}$ mass and $\mathrm{a}_{3/2}>0$ a parameter of order unity which parameterizes our ignorance for the dependence of $|A_\lambda|$ and $|\mathrm{a}_S|$ on $m_{3/2}$. The minimization condition for the total potential in Equation (37a) wrt S leads to a non vanishing $\langle S\rangle$ as follows

$$\frac{d}{dS}\langle V_{\rm tot}(S)\rangle=0\ \ \Rightarrow\ \ \langle S\rangle\simeq{\rm a}_{3/2}m_{3/2}c_-(1-Nr_\pm)/\lambda. \tag{37b}$$

At this S value, $\langle V_{\rm tot}(S)\rangle$ develops a minimum since

$$\frac{d^2}{dS^2}\langle V_{\rm tot}(S)\rangle=\lambda^2M^2/c_-(1-Nr_\pm) \tag{37c}$$

becomes positive for $r_\pm<1/N$, as dictated by Equation (15). Let us emphasize here that SUSY breaking effects explicitly break $U(1)_R$ to the $\mathbb{Z}_2^R$ matter parity, under which all the matter (quark and lepton) superfields change sign. Combining $\mathbb{Z}_2^R$ with the $\mathbb{Z}_2^{\rm f}$ fermion parity, under which all fermions change sign, yields the well-known R-parity. Recall that this residual symmetry prevents the rapid proton decay, guarantees the stability of the lightest SUSY particle (LSP) and therefore, it provides a well-motivated cold dark matter (CDM) candidate. Since S has the R symmetry of W, $\langle S\rangle$ in Equation (37b) breaks also spontaneously $U(1)_R$ to $\mathbb{Z}_2^R$. Thanks to this fact, $\mathbb{Z}_2^R$ remains unbroken and so, no disastrous domain walls are formed.

The generated μ term from the second term in the rhs of Equation (3b) is

$$\mu=\lambda_\mu\langle S\rangle\simeq\lambda_\mu{\rm a}_{3/2}m_{3/2}c_-(1-Nr_\pm)/\lambda \tag{38a}$$

which, taking into account Equation (28), is written as

$$\mu\simeq1.2\times10^2\lambda_\mu{\rm a}_{3/2}m_{3/2}(1-Nr_\pm)r_\pm^{-3/2}f_{n\star}^{-n}\frac{(f_{n\star}-1)^{3/2}}{n(1-f_{n\star})+1}, \tag{38b}$$

where c_- and λ are eliminated. As a consequence, the resulting μ in Equation (38a) depends on $r_\pm$ and n but does not depend on λ and c_-—in contrast to the originally proposed scheme in Reference [73] where a λ dependence remains. Note, also, that λ_μ (and so μ) may have either sign without any essential alteration in the stability analysis of the inflationary system—see Table 3. Thanks to the magnitude of the proportionality constant and given that $r_\pm^{-3/2}$ turns out to be about 10^3 for $r_\pm$ of order 0.01, as indicated by Figure 2, we conclude that any $|\mu|$ value is accessible for the λ_μ values allowed by Equations (18a) and (18b) without any ugly hierarchy between $m_{3/2}$ and μ.

To highlight further the statement above, we can employ Equation (38a) to derive the $m_{3/2}$ values required so as to obtain a specific μ value. E.g., we fix $\mu=1$ TeV as suggested by many MSSM versions

for acceptable low energy phenomenology—see Reference [101]. Given that Equation (38a) dependents on $r_\pm$ and n, which crucially influences n and r, we expect that the required $m_{3/2}$ is a function of n and r as depicted in Figure 3a,b respectively. We take $\lambda_\mu = 10^{-6}$, in accordance with Equations (18a) and (18b), $a_{3/2} = 1$, $K = K_2$ or K_3 with $N_X = 2$ and $n = -0.1$ (dot-dashed line), $n = 0$ (solid line), or $n = +0.1$ (dashed line). Varying $r_\pm$ in the allowed ranges indicated in Figure 2a for any of the n's above we obtain the variation of $m_{3/2}$ solving Equation (38a) wrt $m_{3/2}$. We see that $m_{3/2} \geq 1.6$ TeV with the lowest value obtained for $n = 0.1$. Also, $m_{3/2}$ corresponding to $n = 0$ and -0.1 increases sharply as $r_\pm$ approaches 0.49 due to the denominator $1 - Nr_\pm$ which approaches zero. Had we used $K = K_1$ this enhancement would have been occurred as $r_\pm$ tends to 0.33.

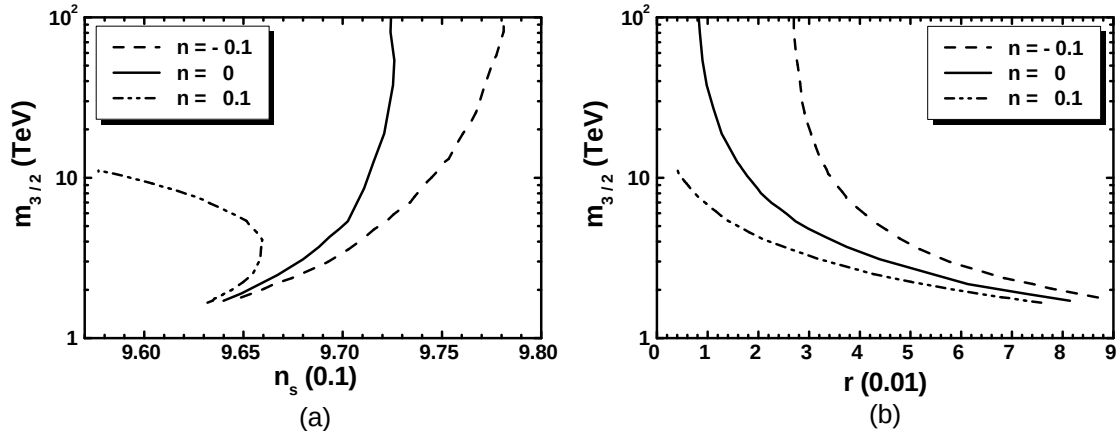

Figure 3. The gravitino mass $m_{3/2}$ versus n_s (**a**) or r (**b**) for $\mu = 1$ TeV, $\lambda_\mu = 10^{-6}$, $a_{3/2} = 1$, $K = K_2$ or K_3 with $N_X = 2$ and $n = -0.1$ (dot-dashed line), $n = 0$ (solid line), or $n = +0.1$ (dashed line).

Obviously the proposed resolution of the μ problem of MSSM relies on the existence of non-zero A_λ and/or a_S. These issues depend on the adopted model of SUSY breaking. Here we have in mind mainly the gravity mediated SUSY breaking without, though, to specify the extra terms in the superpotential and the Kähler potentials which ensure the appropriate soft SUSY breaking parameters and the successful stabilization of the sgolstino—cf. Reference [102,103]. Since this aim goes beyond the framework of this work, we restrict ourselves to assume that these terms can be added without disturbing the inflationary dynamics.

4.3. Connection with the MSSM Phenomenology

Taking advantage from the updated investigation of the parameter space of Constrained MSSM (CMSSM) in Reference [101] we can easily verify that the μ and $m_{3/2}$ values satisfying Equation (38a) are consistent with the values required by the analyses of the low energy observables of MSSM. We concentrate on CMSSM which is the most predictive, restrictive and well-motivated version of MSSM, employing the free parameters

$$\text{sign}\mu, \quad \tan\beta = \langle H_u \rangle / \langle H_d \rangle, \quad M_{1/2}, \quad m_0 \quad \text{and} \quad A_0,$$

where signμ is the sign of μ, and the three last mass parameters denote the common gaugino mass, scalar mass, and trilinear coupling constant, respectively, defined at a high scale which is determined by the unification of the gauge coupling constants. The parameter $|\mu|$ is not free, since it is computed at low scale enforcing the conditions for the electroweak symmetry breaking. The values of these parameters can be tightly restricted imposing a number of cosmo-phenomenological constraints. Namely, these constraints originate from the cold dark matter abundance in the universe and its direct detection experiments, the B-physics, as well as the masses of the sparticles and the lightest neutral

CP-even Higgs boson. Some updated results are recently presented in Reference [101], where we can also find the best-fit values of $|A_0|$, m_0 and $|\mu|$ listed in Table 4. We see that there are four allowed regions characterized by the specific mechanism for suppressing the relic density of the lightest sparticle which can act as dark matter. If we identify m_0 with $m_{3/2}$ and $|A_0|$ with $|A_\lambda| = |a_S|$ we can derive first $a_{3/2}$ and then the λ_μ values which yield the phenomenologically desired $|\mu|$. Here we assume that renormalization effects in the derivation of μ are negligible. For the completion of this calculation we have to fix some sample values of $(n, r_\pm)$. From those shown in Equation (33), we focus on this which is favored from the String theory with $n = 0$ and this which assure central values of the observables in Equations (1) and (31). More explicitly, we consider the following benchmark values:

$$(n, r_\pm) = (0, 0.015) \quad \text{resulting to } (n_s, r) = (0.968, 0.044)\,, \tag{39a}$$

$$(n, r_\pm) = (0.042, 0.025) \quad \text{resulting to } (n_s, r) = (0.968, 0.028)\,. \tag{39b}$$

The outputs of our computation is listed in the two rightmost columns of Table 4. Since the required λ_μ's are compatible with Equations (18a) and (18b) for $N_X = 2$, we conclude that the whole inflationary scenario can be successfully combined with CMSSM. The λ_μ values are lower compared to those found in Reference [54]. Moreover, in sharp contrast to that model, all the CMSSM regions can be consistent with the gravitino limit on $T_{\rm rh}$—see Section 5.2. Indeed, $m_{3/2}$ as low as 1 TeV become cosmologically safe, under the assumption of the unstable $\widetilde{G}$, for the $T_{\rm rh}$ values, necessitated for satisfactory leptogenesis, see Section 5.4. From the analysis above it is evident that the solution of the μ problem in our model becomes a bridge connecting the high with the low-energy phenomenology.

Table 4. The required λ_μ values which render our models compatible with the best-fit points in the CMSSM, as found in Reference [101], for $m_0 = m_{3/2}$, $|A_\lambda| = |a_S| = |A_0|$, $K = K_2$ or K_3 with $N_X = 2$ and $(n, r_\pm)$ given in Equations (39a) and (39b).

CMSSM	$\|A_0\|$	m_0	$\|\mu\|$	$a_{3/2}$	$\lambda_\mu(10^{-6})$ for (n_s,r) in	
Region	**(TeV)**	**(TeV)**	**(TeV)**		**Equation (39a)**	**Equation (39b)**
A/H Funnel	9.9244	9.136	1.409	1.086	0.441	0.6045
$\tilde{\tau}$ Coannihilation	1.2271	1.476	2.62	0.831	6.63	9.1
$\tilde{t}$ Coannihilation	9.965	4.269	4.073	2.33	1.27	1.74
$\tilde{\chi}_1^\pm$ Coannihilation	9.2061	9.000	0.983	1.023	0.332	0.454

5. Non-Thermal Leptogenesis and Neutrino Masses

We below specify how our inflationary scenario makes a transition to the radiation dominated era (Section 5.1) and offers an explanation of the observed BAU (Section 5.2) consistently with the $\widetilde{G}$ constraint and the low energy neutrino data (Section 5.3). Our results are summarized in Section 5.4.

5.1. Inflaton Mass and Decay

The transition to the radiation epoch is controlled by the inflaton mass and its decay channels. These issues are investigated below in Sections 5.1.1 and 5.1.2 respectively.

5.1.1. Mass Spectrum at the SUSY Vacuum

When HI is over, the inflaton continues to roll down towards the SUSY vacuum, Equation (35). Soon after, it settles into a phase of damped oscillations around the minimum of $\widehat{V}_{\rm HI}$. The (canonically normalized) inflaton,

$$\widehat{\delta\phi} = \langle J\rangle \delta\phi \;\; \text{with} \;\; \delta\phi = \phi - M \;\; \text{and} \;\; \langle J\rangle = \sqrt{\langle \kappa_+\rangle} = \sqrt{c_-(1 - N r_\pm)} \tag{40}$$

acquires mass, at the SUSY vacuum in Equation (35), which is given by

$$\widehat{m}_{\delta\phi} = \left\langle \widehat{V}_{\mathrm{HI},\widehat{\phi}\widehat{\phi}} \right\rangle^{1/2} = \left\langle \widehat{V}_{\mathrm{HI},\phi\phi}/J^2 \right\rangle^{1/2} \simeq \frac{\lambda M}{\sqrt{2c_- \left(1 - N r_\pm\right)}}\,, \tag{41}$$

where the last (approximate) equality above is valid only for $r_\pm \ll 1/N$—see Equations (14) and (16b). As we see, $\widehat{m}_{\delta\phi}$ depends crucially on M which may be, in principle, a free parameter acquiring any subplanckian value without disturbing the inflationary process. To determine better our models, though, we prefer to specify M requiring that $\langle\Phi\rangle$ and $\langle\bar{\Phi}\rangle$ in Equation (35) take the values dictated by the unification of the MSSM gauge coupling constants, despite the fact that $U(1)_{B-L}$ gauge symmetry does not disturb this unification and M could be much lower. In particular, the unification scale $M_{\mathrm{GUT}} \simeq 2\times 10^{16}$ GeV can be identified with M_{BL}—see Table 3—at the SUSY vacuum in Equation (35), i.e.,

$$\frac{\sqrt{c_-(\langle f_{\mathcal{R}}\rangle - N r_\pm)}\, g M}{\sqrt{\langle f_{\mathcal{R}}\rangle}} = M_{\mathrm{GUT}} \;\Rightarrow\; M \simeq M_{\mathrm{GUT}}/g\sqrt{c_-\left(1 - N r_\pm\right)}, \tag{42}$$

with $g \simeq 0.7$ being the value of the GUT gauge coupling and we take into account that $\langle f_{\mathcal{R}}\rangle \simeq 1$. Upon substitution of the last expression in Equation (42) into Equation (41) we can infer that $\widehat{m}_{\delta\phi}$ remains constant for fixed n and $r_\pm$ since λ/c_- is fixed too—see Equation (28). Particularly, along the bold solid line in Figure 2b we obtain

$$5.8\times 10^{11} \lesssim \widehat{m}_{\delta\phi}/\mathrm{GeV} \lesssim 3.6\times 10^{13} \quad \text{for } K = K_1; \tag{43}$$

$$5.3\times 10^{10} \lesssim \widehat{m}_{\delta\phi}/\mathrm{GeV} \lesssim 3.6\times 10^{13} \quad \text{for } K = K_2 \text{ and } K_3\,, \tag{44}$$

where the lower [upper] bound is obtained for $(n, r_\pm) = (-0.121, 0.0125)$ [$(n, r_\pm) = (0.0215, 0.499)$ for $K = K_2$ and K_3 or $(n, r_\pm) = (0.0215, 0.33)$ for $K = K_1$]—see Equation (33). We remark that $\widehat{m}_{\delta\phi}$ is heavily affected from the choice of K's in Equations (4a)–(4c) as $r_\pm$ approaches its lower bound in Figure 2a—note that this point is erroneously interpreted in Reference [26]. For any choice of K we observe that $\widehat{m}_{\delta\phi}$ approaches its value within pure nMI [12,13] and Starobinsky inflation [49–51,54] as $r_\pm$ approaches its maximal value in Equation (15)—or as r approaches 0.003.

5.1.2. Inflaton Decay

The decay of $\widehat{\delta\phi}$ is processed through the following decay channels [74]:

(a) Decay channel into N_i^c's.

The lagrangian which describes these decay channels arises from the part of the SUGRA langrangian [104] containing two fermions. In particular,

$$\begin{aligned}\mathcal{L}_{\widehat{\delta\phi}\to N_i^c} &= -\frac{1}{2} e^{K/2m_{\mathrm{P}}^2} W_{\mathrm{HI},N_i^c N_i^c} N_i^c N_i^c + \text{h.c.} = \frac{\lambda_{iN^c}}{2}\left(1 + c_+\frac{\phi^2}{m_{\mathrm{P}}^2}\right)^{-N/2} \phi N_i^c N_i^c + \text{h.c.}\\ &= g_{iN^c}\widehat{\delta\phi}\, N_i^c N_i^c + \cdots \text{ with } g_{iN^c} = \frac{\lambda_{iN^c}}{2\langle J\rangle}\left(1 - 3c_+\frac{N}{2}\frac{M^2}{m_{\mathrm{P}}^2}\right),\end{aligned} \tag{45a}$$

where the masses of N_i^c's are obtained from the third term of the rhs in Equation (3b) as follows

$$M_{iN^c} = \lambda_{iN^c} M/f_{0\mathcal{R}}^{N/2} \quad \text{with} \quad f_{0\mathcal{R}} = 1 + c_+ M^2/m_{\mathrm{P}}^2 \quad \text{and} \quad M_{iN^c} \leq 7.1M\,, \tag{45b}$$

due to the needed perturbativity of λ_{iN^c}, i.e., $\lambda_{iN^c}^2/4\pi \leq 1$. The result in Equation (45a) can be extracted, if we perform an expansion for $m_{\rm P} \to \infty$ and then another about $\langle\phi\rangle$. This channel gives rise to the following decay width

$$\widehat{\Gamma}_{\delta\phi\to N_i^c} = \frac{1}{16\pi} g_{iN^c}^2 \widehat{m}_{\delta\phi} \left(1 - 4M_{iN^c}^2/\widehat{m}_{\delta\phi}^2\right)^{3/2}, \tag{45c}$$

where we take into account that $\widehat{\delta\phi}$ decays into identical particles.

(b) Decay channel into H_u and H_d.

The lagrangian term which describes the relevant interaction comes from the F-term SUGRA scalar potential in Equation (6c). Namely, we obtain

$$\begin{aligned} \mathcal{L}_{\widehat{\delta\phi}\to H_u H_d} &= -e^{K/m_{\rm P}^2} K^{SS^*} |W_{{\rm HI},S}|^2 = -\frac{1}{4}\lambda\lambda_\mu f_{\mathcal{R}}^{-2(n+1)} \left(\phi^2 - M^2\right) H_u^* H_d^* + \cdots \\ &= -g_H \widehat{m}_{\delta\phi} \widehat{\delta\phi} H_u^* H_d^* + \cdots \text{ with } g_H = \frac{\lambda_\mu}{\sqrt{2}} \left(1 - 2c_+(n+1)\frac{M^2}{m_{\rm P}^2}\right), \end{aligned} \tag{46a}$$

where we take into account Equations (10) and (41). This interaction gives rise to the following decay width

$$\widehat{\Gamma}_{\delta\phi\to H} = \frac{2}{8\pi} g_H^2 \widehat{m}_{\delta\phi}, \tag{46b}$$

where we take into account that H_u and H_d are $SU(2)_{\rm L}$ doublets. Equations (18a) and (18b) facilitate the reduction of $\widehat{\Gamma}_{\delta\phi\to H}$ to a level which allows for the decay mode into N_i^c's playing its important role for nTL.

(c) Three-particle decay channels.

Focusing on the same part of the SUGRA langrangian [104] as in paragraph (a), for a typical trilinear superpotential term of the form $W_y = yXYZ$—cf. Equation (3a)—where y is a Yukawa coupling constant, we obtain the interactions described by

$$\begin{aligned} \mathcal{L}_{y\widehat{\delta\phi}} &= -\frac{1}{2} e^{K/2m_{\rm P}^2} \left(W_{y,YZ}\psi_Y\psi_Z + W_{y,XZ}\psi_X\psi_Z + W_{y,XY}\psi_X\psi_Y\right) + \text{h.c.} \\ &= g_y \widehat{\delta\phi} \left(X\psi_Y\psi_Z + Y\psi_X\psi_Z + Z\psi_X\psi_Y\right) + \text{h.c.} \text{ with } g_y = N y_3 c_+ \frac{M}{\langle J\rangle m_{\rm P}}, \end{aligned} \tag{47a}$$

where ψ_X, ψ_Y and ψ_Z are the chiral fermions associated with the superfields X, Y and Z whose the scalar components are denoted with the superfield symbol. Working in the large $\tan\beta$ regime which yields similar y's for the 3rd generation, we conclude that the interaction above gives rise to the following 3-body decay width

$$\widehat{\Gamma}_{\delta\phi\to XYZ} = \frac{n_{\rm f}}{512\pi^3} g_y^2 \frac{\widehat{m}_{\delta\phi}^3}{m_{\rm P}^2}, \tag{47b}$$

where for the third generation we take $y \simeq (0.4 - 0.6)$, computed at the $\widehat{m}_{\delta\phi}$ scale, and $n_{\rm f} = 14$ for $\widehat{m}_{\delta\phi} < M_{3N^c}$—summation is taken over $SU(3)_{\rm C}$ and $SU(2)_{\rm L}$ indices.

Since the decay width of the produced N_i^c is much larger than $\widehat{\Gamma}_{\delta\phi}$ the reheating temperature, $T_{\rm rh}$, is exclusively determined by the inflaton decay and is given by [105]

$$T_{\rm rh} = \left(\frac{72}{5\pi^2 g_*}\right)^{1/4} \sqrt{\widehat{\Gamma}_{\delta\phi} m_{\rm P}} \text{ with } \widehat{\Gamma}_{\delta\phi} = \widehat{\Gamma}_{\delta\phi\to N_i^c} + \widehat{\Gamma}_{\delta\phi\to H} + \widehat{\Gamma}_{\delta\phi\to XYZ}, \tag{48}$$

where $g_* \simeq 228.75$ counts the effective number of relativistic degrees of freedom of the MSSM spectrum at the temperature $T \simeq T_{\rm rh}$.

5.2. Lepton-Number and Gravitino Abundances

The mechanism of nTL [57–59] can be activated by the out-of-equilibrium decay of the N_i^c's produced by the $\widehat{\delta\phi}$ decay, via the interactions in Equation (45a). If $T_{\rm rh} \ll M_{iN^c}$, the out-of-equilibrium condition [52,53] is automatically satisfied. Namely, N_i^c decay into (fermionic and bosonic components of) H_u and L_i via the tree-level couplings derived from the last term in the rhs of Equation (3a). The resulting—see Section 5.3—lepton-number asymmetry ε_i (per N_i^c decay) after reheating can be partially converted via sphaleron effects into baryon-number asymmetry. In particular, the B yield can be computed as

$$Y_B = -0.35 Y_L \quad \text{with} \tag{49a}$$

$$Y_L = 2\frac{5}{4}\frac{T_{\rm rh}}{\widehat{m}_{\delta\phi}}\sum_{i=1}^{3}\frac{\widehat{\Gamma}_{\delta\phi\to N_i^c}}{\widehat{\Gamma}_{\delta\phi}}\varepsilon_i\,. \tag{49b}$$

The numerical factor in the rhs of Equation (49a) comes from thesphaleron effects, whereas the one (5/4) in the rhs of Equation (49b) is due to the slightly different calculation [105] of $T_{\rm rh}$—cf. Reference [52,53]. The validity of the formulae above requires that the $\widehat{\delta\phi}$ decay into a pair of N_i^c's is kinematically allowed for at least one species of the N_i^c's and also that there is no erasure of the produced Y_L due to N_1^c mediated inverse decays and $\Delta L = 1$ scatterings [106]. Theses prerequisites are ensured if we impose

$$\widehat{m}_{\delta\phi} \geq 2M_{1N^c} \tag{50a}$$

$$\text{and } M_{1N^c} \gtrsim 10 T_{\rm rh}. \tag{50b}$$

Finally, the interpretation of BAU through nTL dictates [56] at 95% c.l.

$$Y_B = \left(8.64^{+0.15}_{-0.16}\right)\times 10^{-11}. \tag{51}$$

The $T_{\rm rh}$'s required for successful nTL must be compatible with constraints on the $\widetilde{G}$ abundance, $Y_{3/2}$, at the onset of nucleosynthesis (BBN). Assuming that $\widetilde{G}$ is much heavier than the gauginos of MSSM, $Y_{3/2}$ is estimated to be [62–67]

$$Y_{3/2} \simeq 1.9\times 10^{-22} T_{\rm rh}/{\rm GeV}, \tag{52}$$

where we take into account only the thermal $\widetilde{G}$ production. Non-thermal contributions to $Y_{3/2}$ [74] are also possible but strongly dependent on the mechanism of soft SUSY breaking. Moreover, no precise computation of this contribution exists within HI adopting the simplest Polonyi model of SUSY breaking [68,69]. For these reasons, we here adopt the conservative estimation of $Y_{3/2}$ in Equation (52). Nonetheless, it is notable that the non-thermal contribution to $Y_{3/2}$ in models with stabilizer field, as in our case, is significantly suppressed compared to the thermal one.

On the other hand, $Y_{3/2}$ is bounded from above in order to avoid spoiling the success of the BBN. For the typical case where $\widetilde{G}$ decays with a tiny hadronic branching ratio, we have [64–67]

$$Y_{3/2} \lesssim \begin{cases} 10^{-15} \\ 10^{-14} \\ 10^{-13} \\ 10^{-12} \end{cases} \quad \text{for} \quad m_{3/2} \simeq \begin{cases} 0.43\ {\rm TeV} \\ 0.69\ {\rm TeV} \\ 10.6\ {\rm TeV} \\ 13.5\ {\rm TeV} \end{cases} \quad \text{implying} \quad T_{\rm rh} \lesssim 5.3\cdot \begin{cases} 10^6\ {\rm GeV}\,, \\ 10^7\ {\rm GeV}\,, \\ 10^8\ {\rm GeV}\,, \\ 10^9\ {\rm GeV}\,. \end{cases} \tag{53}$$

The bounds above can be somehow relaxed in the case of a stable $\widetilde{G}$—see e.g., Reference [107–110]. In a such case, $\widetilde{G}$ should be the LSP and has to be compatible with the data [56] on the CDM abundance in the universe. To activate this scenario we need lower $m_{3/2}$'s than those obtained in Section 4.2.

As shown from Equation (38b), this result can be achieved for lower μ's and/or larger $a_{3/2}$'s. Low $r_\pm$'s, implying large r's, generically help in this direction too.

Note, finally, that both Equations (49) and (52) calculate the correct values of the B and $\widetilde{G}$ abundances provided that no entropy production occurs for $T < T_{\rm rh}$. This fact can be achieved if the Polonyi-like field z decays early enough without provoking a late episode of secondary reheating. A subsequent difficulty is the possible over-abundance of the CDM particles which are produced by the z decay—see Reference [111–113].

5.3. Lepton-Number Asymmetry and Neutrino Masses

As mentioned above, the decay of $\widetilde{N}^c_i$, emerging from the $\widehat{\delta\phi}$ decay, can generate a lepton asymmetry, ε_i, caused by the interference between the tree and one-loop decay diagrams, provided that a CP-violation occurs in h_{ijN}'s. The produced ε_i can be expressed in terms of the Dirac mass matrix of ν_i, $m_{\rm D}$, defined in the N^c_i-basis, as follows [114–116]:

$$\varepsilon_i = \frac{\sum_{j\neq i} {\rm Im}\left[(m^\dagger_{\rm D} m_{\rm D})^2_{ij}\right]}{8\pi \langle H_u\rangle^2 (m^\dagger_{\rm D} m_{\rm D})_{ii}} \left(F_{\rm S}\left(x_{ij}, y_i, y_j\right) + F_{\rm V}(x_{ij})\right), \tag{54a}$$

where we take $\langle H_u\rangle \simeq 174$ GeV, for large $\tan\beta$ and

$$x_{ij} = \frac{M_{jN^c}}{M_{iN^c}}, \;\; F_{\rm V}(x) = -x\ln\left(1+x^{-2}\right) \;\; \text{and} \;\; F_{\rm S}(x) = \frac{-2x}{x^2-1}\cdot \tag{54b}$$

The involved in Equation (54a) $m_{\rm D}$ can be diagonalized if we define a basis—called *weak basis* henceforth—in which the lepton Yukawa couplings and the $SU(2)_{\rm L}$ interactions are diagonal in the space of generations. In particular we have

$$U^\dagger m_{\rm D} U^{c\dagger} = d_{\rm D} = {\rm diag}\left(m_{1{\rm D}}, m_{2{\rm D}}, m_{3{\rm D}}\right), \tag{55}$$

where U and U^c are 3×3 unitary matrices which relate L_i and N^c_i (in the N^c_i-basis) with the ones L'_i and $\nu^{c\prime}_i$ in the weak basis as follows

$$L' = LU \;\; \text{and} \;\; N^{c\prime} = U^c N^c. \tag{56}$$

Here, we write LH lepton superfields, i.e., $SU(2)_{\rm L}$ doublet leptons, as row 3-vectors in family space and RH anti-lepton superfields, i.e., $SU(2)_{\rm L}$ singlet anti-leptons, as column 3-vectors. Consequently, the combination $m^\dagger_{\rm D} m_{\rm D}$ appeared in Equation (54a) turns out to be a function just of $d_{\rm D}$ and U^c. Namely,

$$m^\dagger_{\rm D} m_{\rm D} = U^{c\dagger} d_{\rm D} d_{\rm D} U^c. \tag{57}$$

The connection of the leptogenesis scenario with the low energy neutrino data can be achieved through the seesaw formula, which gives the light-neutrino mass matrix m_ν in terms of $m_{i{\rm D}}$ and M_{iN^c}. Working in the N^c_i-basis, we have

$$m_\nu = -m_{\rm D}\, d^{-1}_{N^c}\, m^{\rm T}_{\rm D}, \tag{58}$$

where

$$d_{N^c} = {\rm diag}\left(M_{1N^c}, M_{2N^c}, M_{3N^c}\right) \tag{59}$$

with $M_{1N^c} \leq M_{2N^c} \leq M_{3N^c}$ real and positive. Solving Equation (55) wrt $m_{\rm D}$ and inserting the resulting expression in Equation (58) we extract the mass matrix

$$\bar{m}_\nu = U^\dagger m_\nu U^* = -d_{\rm D} U^c d^{-1}_{N^c} U^{c{\rm T}} d_{\rm D}, \tag{60a}$$

which can be diagonalized by the unitary PMNS matrix satisfying

$$\bar{m}_\nu = U_\nu^* \,\mathrm{diag}\,(m_{1\nu}, m_{2\nu}, m_{3\nu})\; U_\nu^\dagger, \tag{60b}$$

and parameterized as follows

$$U_\nu = \begin{pmatrix} c_{12}c_{13} & s_{12}c_{13} & s_{13}e^{-i\delta} \\ -c_{23}s_{12} - s_{23}c_{12}s_{13}e^{i\delta} & c_{23}c_{12} - s_{23}s_{12}s_{13}e^{i\delta} & s_{23}c_{13} \\ s_{23}s_{12} - c_{23}c_{12}s_{13}e^{i\delta} & -s_{23}c_{12} - c_{23}s_{12}s_{13}e^{i\delta} & c_{23}c_{13} \end{pmatrix} \cdot \mathrm{diag}\left(e^{-i\varphi_1/2}, e^{-i\varphi_2/2}, 1\right), \tag{60c}$$

where $c_{ij} := \cos\theta_{ij}$, $s_{ij} := \sin\theta_{ij}$ and δ, φ_1 and φ_2 are the CP-violating Dirac and Majorana phases.

Following a bottom-up approach, along the lines of References [54,55,106,117], we can find $\bar{m}_\nu$ via Equation (60b) adopting the normal or inverted hierarchical scheme of neutrino masses. In particular, $m_{i\nu}$'s can be determined via the relations

$$m_{2\nu} = \sqrt{m_{1\nu}^2 + \Delta m_{21}^2} \;\text{ and }\; \begin{cases} m_{3\nu} = \sqrt{m_{1\nu}^2 + \Delta m_{31}^2}, & \text{for normally ordered (NO) } m_\nu\text{'s} \\ \quad\text{or} & \\ m_{1\nu} = \sqrt{m_{3\nu}^2 + |\Delta m_{31}^2|}, & \text{for invertedly ordered (IO) } m_\nu\text{'s,} \end{cases} \tag{61}$$

where the neutrino mass-squared differences Δm_{21}^2 and Δm_{31}^2 are listed in Table 5 and computed by the solar, atmospheric, accelerator and reactor neutrino experiments. We also arrange there the inputs on the mixing angles θ_{ij} and on the CP-violating Dirac phase, δ, for normal [inverted] neutrino mass hierarchy [70]—see also Reference [71,72]. Moreover, the sum of $m_{i\nu}$'s is bounded from above by the current data [56], as follows

$$\textstyle\sum_i m_{i\nu} \leq 0.23 \text{ eV} \;\text{ at 95\% c.l.} \tag{62}$$

Table 5. Low energy experimental neutrino data for normal or inverted hierarchical neutrino masses.

Parameter	Best Fit $\pm 1\sigma$	
	Normal	Inverted
	Hierarchy	
$\Delta m_{21}^2/10^{-3}\text{eV}^2$	$7.6^{+0.19}_{-0.18}$	
$\Delta m_{31}^2/10^{-3}\text{eV}^2$	$2.48^{+0.05}_{-0.07}$	$2.38^{+0.05}_{-0.06}$
$\sin^2\theta_{12}/0.1$	3.23 ± 0.16	
$\sin^2\theta_{13}/0.01$	2.26 ± 0.12	2.29 ± 0.12
$\sin^2\theta_{23}/0.1$	$5.67^{+0.32}_{-1.24}$	$5.73^{+0.25}_{-0.39}$
δ/π	$1.41^{+0.55}_{-0.4}$	1.48 ± 0.31

Taking also $m_{i\mathrm{D}}$ as input parameters we can construct the complex symmetric matrix

$$\mathbb{W} = -d_\mathrm{D}^{-1}\bar{m}_\nu d_\mathrm{D}^{-1} = U^c d_{N^c} U^{c\mathsf{T}}, \tag{63a}$$

see Equation (60a)—from which we can extract d_{N^c} as follows

$$d_{N^c}^{-2} = U^{c\dagger}\mathbb{W}\mathbb{W}^\dagger U^c\,. \tag{63b}$$

Note that $\mathbb{W}\mathbb{W}^\dagger$ is a 3×3 complex, hermitian matrix and can be diagonalized numerically so as to determine the elements of U^c and the M_{iN^c}'s. We then compute m_D through Equation (57) and the ε_i's through Equation (54a).

5.4. Results

The success of our inflationary scenario can be judged, if, in addition to the constraints of Section 3.3, it can become consistent with the post-inflationary requirements mentioned in Sections 5.2 and 5.3. More specifically, the quantities which have to be confronted with observations are Y_B and $Y_{3/2}$ which depend on $\widehat{m}_{\delta\phi}$, $T_{\rm rh}$, M_{iN^c} and $m_{i\rm D}$'s —see Equations (49) and (52). As shown in Equation (41), $\widehat{m}_{\delta\phi}$ is a function of n and $r_\pm$ whereas $T_{\rm rh}$ in Equation (48) depend on λ_μ, y and the masses of the N_i^c's into which $\widehat{\delta\phi}$ decays. Throughout our computation we fix $y = 0.5$ which is a representative value. Also, when we employ $K = K_1$ and K_2 we take $N_X = 2$ which allows for a quite broad available λ_μ margin. As regards the ν_i masses, we follow the bottom-up approach described in Section 5.3, according to which we find the M_{iN^c}'s by using as inputs the $m_{i\rm D}$'s, a reference mass of the ν_i's – $m_{1\nu}$ for NO $m_{i\nu}$'s, or $m_{3\nu}$ for IO $m_{i\nu}$'s –, the two Majorana phases φ_1 and φ_2 of the PMNS matrix, and the best-fit values, listed in Table 5, for the low energy parameters of neutrino physics. In our numerical code, we also estimate, following Reference [118], the RG evolved values of the latter parameters at the scale of nTL, $\Lambda_L = \widehat{m}_{\delta\phi}$, by considering the MSSM with $\tan\beta \simeq 50$ as an effective theory between Λ_L and the soft SUSY breaking scale, $M_{\rm SUSY} = 1.5$ TeV. We evaluate the M_{iN^c}'s at Λ_L, and we neglect any possible running of the $m_{i\rm D}$'s and M_{iN^c}'s. The so obtained M_{iN^c}'s clearly correspond to the scale Λ_L.

We start the exposition of our results arranging in Table 6 some representative values of the parameters which yield Y_B and $Y_{3/2}$ compatible with Equations (51) and (53), respectively. We set $\lambda_\mu = 10^{-6}$ in accordance with Equations (18a) and (18b). Also, we select the $(n, r_\pm)$ value in Equation (39b) which ensures central n and r in Equations (1) and (31a). We obtain $M = 2.39 \times 10^{15}$ GeV and $\widehat{m}_{\delta\phi} = 8.8 \times 10^{10}$ GeV for $K = K_1$ or $M = 2.43 \times 10^{15}$ GeV and $\widehat{m}_{\delta\phi} = 8.6 \times 10^{10}$ GeV for $K = K_2$ or K_3. Although such uncertainties from the choice of K's do not cause any essential alteration of the final outputs, we mention just for definiteness that we take $K = K_2$ or K_3 throughout. We consider NO (cases A and B), almost degenerate (cases C, D and E) and IO (cases F and G) $m_{i\nu}$'s. In all cases, the current limit of Equation (62) is safely met—in the case D this limit is almost saturated. We observe that with NO or IO $m_{i\nu}$'s, the resulting M_{1N^c} and M_{2N^c} are of the same order of magnitude, whereas these are more strongly hierarchical with degenerate $m_{i\nu}$'s. In all cases, the upper bounds in Equation (45b) is preserved thanks to the third term adopted in the rhs of Equation (3b)—cf. Reference [12,13]. We also remark that $\widehat{\delta\phi}$ decays mostly into N_1^c's—see cases A–D. From the cases E–G, where the decay of $\widehat{\delta\phi}$ into N_2^c is unblocked, we notice that, besides case E, the channel $\widehat{\delta\phi} \to N_1^c N_1^c$ yields the dominant contribution to the calculation Y_B from Equation (49), since $\widehat{\Gamma}_{\delta\phi\to N_1^c} \geq \widehat{\Gamma}_{\delta\phi\to N_2^c}$. We observe, however, that $\widehat{\Gamma}_{\delta\phi\to N_i^c} < \widehat{\Gamma}_{\delta\phi\to H}$ ($\widehat{\Gamma}_{\delta\phi\to XYZ}$ is constantly negligible) and so the ratios $\widehat{\Gamma}_{\delta\phi\to N_i^c}/\widehat{\Gamma}_{\delta\phi}$ introduce a considerable reduction in the derivation of Y_B. This reduction could have been eluded, if we had adopted—as in References [12,13,117]—the resolution of the μ problem proposed in Reference [119] since then, the decay mode in Equation (46a) would have disappeared. This proposal, though, is based on the introduction of a Peccei-Quinn symmetry, and so the massless during HI axion generates possibly CDM isocurvature perturbation which is severely restricted by the *Planck* results [56]. In Table 6 we also display, for comparison, the B yield with (Y_B) or without (Y_B^0) taking into account the renormalization group running of the low energy neutrino data. We observe that the two results are in most cases close to each other with the largest discrepancies encountered in cases C, E and F. Shown are also the values of $T_{\rm rh}$, the majority of which are close to 3×10^7 GeV, and the corresponding $Y_{3/2}$'s, which are consistent with Equation (53) for $m_{3/2} \gtrsim 1$ TeV. These values are in nice agreement with the ones needed for the solution of the μ problem of MSSM—see, e.g., Figure 3 and Table 4.

The gauge symmetry considered here does not predict any particular Yukawa unification pattern and so, the $m_{i\rm D}$'s are free parameters. For the sake of comparison, however, we mention that the simplest realization of a SUSY Left-Right [Pati-Salam] GUT predicts [117,120] $h_{iN} = h_{iE}$ [$m_{i\rm D} = m_{iU}$], where m_{iU} are the masses of the up-type quarks and we ignore any possible mixing between generations—these predictions may be eluded though in more realistic implementations of these models

as in References [117,120]. Taking into account the SUSY threshold corrections [91] in the context of MSSM with universal gaugino masses and $\tan\beta \simeq 50$, these predictions are translated as follows

$$\left(m^0_{1\mathrm{D}}, m^0_{2\mathrm{D}}, m^0_{3\mathrm{D}}\right) \simeq \begin{cases} (0.023, 4.9, 100)\ \mathrm{GeV} & \text{for a Left-Right GUT,} \\ (0.0005, 0.24, 100)\ \mathrm{GeV} & \text{for a Pati-Salam GUT.} \end{cases} \tag{64}$$

Comparing these values with those listed in Table 6, we remark that our model is not compatible with any pattern of large hierarchy between the $m_{i\mathrm{D}}$'s, especially in the two lighter generations, since and $m_{1\mathrm{D}} \gg m^0_{1\mathrm{D}}$. On the other hand, $m_{2\mathrm{D}}$ is of the order of $m^0_{2\mathrm{D}}$ in cases A–E whereas $m_{3\mathrm{D}} \simeq m^0_{3\mathrm{D}}$ only in case A. This arrangement can be understood, if we take into account that $m_{1\mathrm{D}}$ and $m_{2\mathrm{D}}$ separately influence the derivation of M_{1N^c} and M_{2N^c} correspondingly—see, e.g., References [12,13,106]. Consequently, the displayed $m_{1\mathrm{D}}$'s assist us to obtain the ε_1's required by Equation (51).

Table 6. Parameters yielding the correct Y_B for various neutrino mass schemes. We take $K = K_2$ or K_3 with $N_X = 2$, $(n, r_\pm)$ in Equation (39b), $\lambda_\mu = 10^{-6}$ and $y = 0.5$.

Parameters	**Cases**						
	A	**B**	**C**	**D**	**E**	**F**	**G**
	Normal Hierarchy			**Almost Degeneracy**		**Inverted Hierarchy**	
Low Scale Parameters							
$m_{1\nu}/0.1$ eV	0.05	0.1	0.5	0.7	0.7	0.5	0.49
$m_{2\nu}/0.1$ eV	0.1	0.13	0.51	0.7	0.7	0.51	0.5
$m_{3\nu}/0.1$ eV	0.5	0.51	0.7	0.86	0.5	0.1	0.05
$\sum_i m_{i\nu}/0.1$ eV	0.65	0.74	1.7	2.3	1.9	1.1	1
φ_1	$-\pi/8$	$-\pi$	π	$\pi/2$	0	0	π
φ_2	π	0	$\pi/3$	$-\pi$	$-\pi/2$	$-\pi/3$	$-\pi/3$
Leptogenesis-Scale Parameters							
$m_{1\mathrm{D}}/0.1$ GeV	2	2.37	10	7.3	4	15	12
$m_{2\mathrm{D}}/$GeV	2.2	1.3	7.5	5	9	0.9	0.9
$m_{3\mathrm{D}}/$GeV	100	250	170	250	1.3	180	270
$M_{1N^c}/10^{10}$ GeV	2.33	1.3	2.97	0.9	0.28	3.11	2.93
$M_{2N^c}/10^{10}$ GeV	7.8	4.5	92.7	137.6	2.4	3.76	3.16
$M_{3N^c}/10^{14}$ GeV	2.9	10.4	2.3	1.1	9.2×10^{-3}	13.8	51.9
Open Decay Channels of the Inflaton, $\widehat{\delta\phi}$, Into N^c_i							
$\widehat{\delta\phi} \to$	N^c_1	N^c_1	N^c_1	N^c_1	$N^c_{1,2}$	$N^c_{1,2}$	$N^c_{1,2}$
$\sum_i \widehat{\Gamma}_{\delta\phi\to N^c_i}/\widehat{\Gamma}_{\delta\phi}$ (%)	16.5	8.2	16.9	4.5	17	22.5	28.3
Resulting B-Yield							
$10^{11} Y^{(0)}_B$	9.5	9.2	6.6	9.2	10.3	6.6	9.3
$10^{11} Y_B$	8.67	8.68	8.6	8.65	8.65	8.72	8.78
Resulting T_{rh} and $\widetilde{G}$-Yield							
$T_{\mathrm{rh}}/10^7$ GeV	2.8	2.7	2.83	2.78	2.83	2.93	3
$10^{15} Y_{3/2}$	5.4	5.1	5.4	5.3	5.4	5.56	5.78

In order to investigate the robustness of the conclusions inferred from Table 6, we examine also how the central value of Y_B in Equation (51) can be achieved by varying $m_{1\mathrm{D}}$ as a function of λ_μ and $\widehat{m}_{\delta\phi}$ in Figure 4a,b respectively. Since the range of Y_B in Equation (51) is very narrow, the 95% c.l. width of these contours is negligible. The convention adopted for these lines is also described in each

plot. In particular, we use solid, dashed, dot-dashed, double dot-dashed and dotted line when the inputs—i.e., m_{iv}, m_{2D}, m_{3D}, φ_1 and φ_2—correspond to the cases B, C, E, D and G of Table 6, respectively. In both graphs we employ $K = K_2$ or K_3 with $N_X = 2$ and $y = 0.5$.

In Figure 4a we fix $(n, r_\pm)$ to the value used in Table 6. Increasing λ_μ above its value shown in Table 6 the ratio $\widehat{\Gamma}_{\delta\phi\to N_i^c}/\widehat{\Gamma}_{\delta\phi}$ gets lower and an increase of M_{1N^c}—and consequently on m_{1D}—is required to keep Y_B at an acceptable level. As a byproduct, $T_{\rm rh}$ and $Y_{3/2}$ increase too and jeopardize the fulfillment of Equation (53). Actually, along the depicted contours in Figure 4a, we obtain $0.04 \leq T_{\rm rh}/10^8 \text{ GeV} \leq 1.5$ whereas the resulting M_{1N^c}'s [M_{2N^c}'s] vary in the ranges (0.8–3) $\times 10^{10}$ GeV, (0.4–2) $\times 10^{10}$ GeV and (2.9–3.1) $\times 10^{10}$ GeV, [(4–6) $\times 10^{10}$ GeV, 1.3 $\times 10^{12}$ GeV and (3–4) $\times 10^{10}$ GeV] for the inputs of cases B, D and G respectively. Finally, M_{3N^c} remains close to its values presented in the corresponding cases of Table 6. At the upper [lower] termination points of the contours, we obtain Y_B lower [upper] that the value in Equation (51).

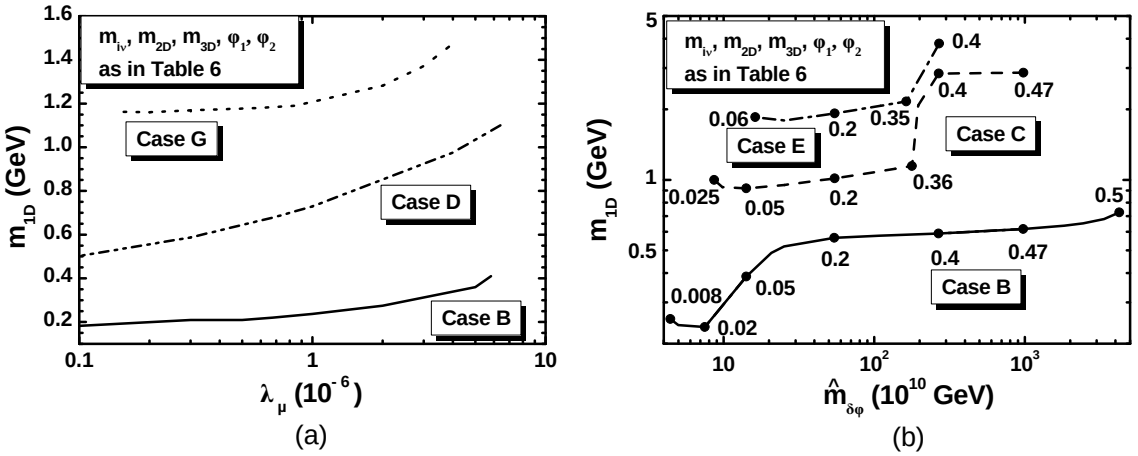

Figure 4. Contours, yielding the central Y_B in Equation (51) consistently with the inflationary requirements, in (**a**) $\lambda_\mu - m_{1D}$ plane for $(n, r_\pm) = (0.042, 0.025)$; (**b**) $\widehat{m}_{\delta\phi} - m_{1D}$ plane for $n = 0$ and $r_\pm$ values indicated on the curves. We also take $K = K_2$ or K_3 with $N_X = 2$, $y = 0.5$ and the values of m_{iv}, m_{2D}, m_{3D}, φ_1 and φ_2 which correspond to the cases B (solid line), C (dashed line), D (double dot-dashed line), E (dot-dashed line), and G (dotted line) of Table 6.

In Figure 4b we fix $n = 0$ and vary $r_\pm$ in the allowed range indicated in Figure 2a. Only some segments from that range fulfill the post-inflationary requirements, despite the fact that the Majorana phases in Table 6 are selected so as to maximize somehow the relevant $\widehat{m}_{\delta\phi}$ margin. Namely, as inferred by the numbers indicated on the curves in the $\widehat{m}_{\delta\phi} - m_{1D}$ plane, we find that $r_\pm$ may vary in the ranges (0.008–0.499), (0.025–0.47) and (0.06–0.4) for the inputs of cases B, C and E respectively. The lower limit on these curves comes from the fact that Y_B is larger than the expectations in Equation (51). At the other end, Equation (50b) is violated and, therefore, washout effects start becoming significant. At these upper termination points of the contours, we obtain $T_{\rm rh}$ of the order 10^9 GeV or $Y_{3/2} > 10^{-13}$ and so, we expect that the constraint of Equation (53) will cut any possible extension of the curves beyond these termination points that could survive the possible washout of Y_L. As induced by Equations (41) and (42), $\widehat{m}_{\delta\phi}$ increases with $r_\pm$ and so, an enhancement of M_{1N^c}'s and similarly of m_{1D}'s is required so that Y_B meets Equation (51). The enhancement of m_{1D} becomes sharp until the point at which the decay channel of $\widehat{\delta\phi}$ into N_2^c's rendered kinematically allowed.

Compared to the findings of the same analysis in other inflationary settings [12,13,54,55], the present scenario is advantageous since $\widehat{m}_{\delta\phi}$ is allowed to reach lower values. Recall—see Section 5.1—that the constant value of $\widehat{m}_{\delta\phi}$ obtained in the papers above represents here the upper bound of $\widehat{m}_{\delta\phi}$ which is approached when $r_\pm$ tends to its maximal value in Equation (15). In practice, this fact offers us the flexibility to reduce $T_{\rm rh}$ and $Y_{3/2}$ at a level compatible with $m_{3/2}$ values as light as 1 TeV which are

excluded elsewhere. On the other hand, Y_B increases when $\widehat{m}_{\delta\phi}$ decreases and can be kept in accordance with the expectations due to variation of $m_{i\mathrm{D}}$ and M_{iN^c}. As a bottom line, nTL not only is a realistic possibility within our models but also it can be comfortably reconciled with the $\widetilde{G}$ constraint.

6. Conclusions

We investigated the realization of kinetically modified non-minimal HI (i.e., Higgs Inflation) and nTL (i.e., non-thermal leptogenesis) in the framework of a model which emerges from MSSM if we extend its gauge symmetry by a factor $U(1)_{B-L}$ and assume that this symmetry is spontaneously broken at a GUT scale determined by the running of the three gauge coupling constants. The model is tied to the super- and Kähler potentials given in Equations (3b) and (4a)–(4c). Prominent in this setting is the role of a softly broken shift-symmetry whose violation is parameterized by the quantity $r_\pm = c_+/c_-$. Combined variation of $r_\pm$ and n —defined in Equation (10)—in the ranges of Equation (33) assists in fitting excellently the present observational data and obtain r's which may be tested in the near future. Moreover, within our model, the μ problem of the MSSM is resolved via a coupling of the stabilizer field (S) to the electroweak higgses, provided that the relevant coupling constant, λ_μ, is relatively suppressed. It is gratifying that the derived relation between μ and $m_{3/2}$ is compatible with successful low energy phenomenology of CMSSM. During the reheating phase that follows HI, the inflaton can decay into N_i^c's (i.e., right-handed neutrinos) allowing, thereby for nTL to occur via the subsequent decay of N_i^c's. Although other decay channels to the MSSM particles via non-renormalizable interactions are also activated, we showed that the generation of the correct Y_B, required by the observations BAU, can be reconciled with the inflationary constraints, the neutrino oscillation parameters and the $\widetilde{G}$ abundance, for masses of the (unstable) $\widetilde{G}$ as light as 1 TeV. More specifically, we found that only N_1^c and N_2^c with masses lower than 1.8×10^{13} GeV can be produced by the inflaton decay which leads to a reheating temperature T_{rh} as low as 2.7×10^7 GeV.

Conflicts of Interest: The author declares no conflict of interest.

References

1. Guth, A.H. The Inflationary Universe: A Possible Solution to the Horizon and Flatness Problems. *Phys. Rev. D* **1981**, *23*, 347–356.
2. Linde, A.D. A New Inflationary Universe Scenario: A Possible Solution of the Horizon, Flatness, Homogeneity, Isotropy and Primordial Monopole Problems. *Phys. Lett. B* **1982**, *108*, 389–393.
3. Albrecht, A.; Steinhardt, P.J. Cosmology for Grand Unified Theories with Radiatively Induced Symmetry Breaking. *Phys. Rev. Lett.* **1982**, *48*, 1220–1223.
4. Salopek, D.S.; Bond, J.R.; Bardeen, J.M. Designing Density Fluctuation Spectra in Inflation. *Phys. Rev. D* **1989**, *40*, 1753–1788.
5. Cervantes-Cota, J.L.; Dehnen, H. Induced gravity inflation in the SU(5) GUT. *Phys. Rev. D* **1995**, *51*, 395–404.
6. Dvali, G.; Shafi, Q.; Schaefer, R. Large scale structure and supersymmetric inflation without fine tuning. *Phys. Rev. Lett.* **1994**, *73*, 1886–1889.
7. Covi, L.; Mangano, A.; Masiero, G.M. Hybrid inflation from supersymmetric SU(5). *Phys. Lett. B* **1998**, *424*, 253–258.
8. Kyae, B.; Shafi, Q. Inflation with realistic supersymmetric SO(10). *Phys. Rev. D* **2005**, *72*, 063515.
9. Kyae, B.; Shafi, Q. Flipped SU(5) predicts delta T/T. *Phys. Lett. B* **2006**, *635*, 247–252.
10. Jeannerot, R.; Khalil, S.; Lazarides, G. New shifted hybrid inflation. *J. High Energy Phys.* **2002**, *2002*, 069.
11. Buchmüller, W.; Domcke, V.; Schmitz, K. Spontaneous B-L Breaking as the Origin of the Hot Early Universe. *Nucl. Phys. B* **2012**, *862*, 587–632.
12. Pallis, C.; Toumbas, N. Non-Minimal Higgs Inflation and non-Thermal Leptogenesis in A Supersymmetric Pati-Salam Model. *J. Cosmol. Astropart. Phys.* **2011**, *2011*, 002.
13. Pallis, C.; Toumbas, N. Leptogenesis and Neutrino Masses in an Inflationary SUSY Pati-Salam Model. In *Open Questions in Cosmology;* Olmo, G.J., Ed.; InTech: Rijeka, Croatia, 2012; pp. 241–269.

14. Antusch, S.; Bastero-Gil, M.; Baumann, J.P.; Dutta, K.; King, S.F.; Kostka, P.M. Gauge Non-Singlet Inflation in SUSY GUTs. *J. High Energy Phys.* **2010**, *2010*, 100.
15. Nakayama, K.; Takahashi, F. PeV-scale Supersymmetry from New Inflation. *J. Cosmol. Astropart. Phys.* **2012**, *2012*, 035.
16. Einhorn, M.B.; Jones, D.R.T. GUT Scalar Potentials for Higgs Inflation. *J. Cosmol. Astropart. Phys.* **2012**, *2012*, 049.
17. Heurtier, L.; Khalil, S.; Moursy, A. Single Field Inflation in Supergravity with a U(1) Gauge Symmetry. *J. Cosmol. Astropart. Phys.* **2015**, *2015*, 045.
18. Leontaris, G.K.; Okada, N.; Shafi, Q. Non-minimal quartic inflation in supersymmetric SO(10). *Phys. Lett. B* **2017**, *2017*, 256–259.
19. Arai, M.; Kawai, S.; Okada, N. Higgs inflation in minimal supersymmetric SU(5) grand unified theory. *Phys. Rev. D* **2011**, *84*, 123515.
20. Ellis, J.; He, H.J.; Xianyu, Z.Z. New Higgs Inflation in a No-Scale Supersymmetric SU(5) GUT. *Phys. Rev. D* **2015**, *91*, 021302.
21. Ellis, J.; He, H.J.; Xianyu, Z.Z. Higgs Inflation, Reheating and Gravitino Production in No-Scale Supersymmetric GUTs. *J. Cosmol. Astropart. Phys.* **2016**, *2016*, 068.
22. Kawai, S.; Kim, J. Multifield dynamics of supersymmetric Higgs inflation in SU(5) GUT. *Phys. Rev. D* **2016**, *2016*, 065023.
23. Ellis, J.; Garcia, M.A.G.; Nagata, N.; Nanopoulos, D.V.; Olive, K.A. Starobinsky-Like Inflation and Neutrino Masses in a No-Scale SO(10) Model. *J. Cosmol. Astropart. Phys.* **2016**, *2016*, 018.
24. Ellis, J.; Garcia, M.A.G.; Nagata, N.; Nanopoulos, D.V.; Olive, K.A. Starobinsky-like Inflation, Supercosmology and Neutrino Masses in No-Scale Flipped SU(5). *J. Cosmol. Astropart. Phys.* **2017**, *2017*, 006.
25. Pallis, C. Kinetically modified nonminimal Higgs inflation in supergravity. *Phys. Rev. D* **2015**, *92*, 121305.
26. Pallis, C. Variants of Kinetically Modified Non-Minimal Higgs Inflation in Supergravity. *J. Cosmol. Astropart. Phys.* **2016**, *2016*, 037.
27. Pallis, C. Kinetically modified nonminimal chaotic inflation. *Phys. Rev. D* **2015**, *91*, 123508.
28. Pallis, C. Observable Gravitational Waves from Kinetically Modified Non-Minimal Inflation. *PoS PLANCK* **2015**, *2015*, 095.
29. Takahashi, F. Linear Inflation from Running Kinetic Term in Supergravity. *Phys. Lett. B* **2010**, *693*, 140–143.
30. Nakayama, K.; Takahashi, F. Running Kinetic Inflation. *J. Cosmol. Astropart. Phys.* **2010**, *2010*, 009.
31. Lee, H.M. Chaotic inflation and unitarity problem. *Eur. Phys. J. C* **2014**, *74*, 3022.
32. Pallis, C. Non-Minimally Gravity-Coupled Inflationary Models. *Phys. Lett. B* **2010**, *692*, 287–296.
33. Kallosh, R.; Linde, A.; Roest, D. Universal Attractor for Inflation at Strong Coupling. *Phys. Rev. Lett.* **2014**, *112*, 011303.
34. Ade, P.A.R.; Aghanim, N.; Arnaud, M.; Arroja, F.; Ashdown, M.; Aumont, J.; Baccigalupi, C.; Balladini, M.; Banday, A.J.; Barreiro, R.B.; et al. Planck 2015 results. XX. Constraints on inflation. *Astron. Astrophys.* **2016**, *594*, A20.
35. Ade, P.A.R.; Aikin, R.W.; Bock, J.J.; Brevik, J.A.; Filippini, J.P.; Hui, H.; Kefeli, S.; Lueker, M.; O'Brient, R.; Orlando, A.; et al. Improved Constraints on Cosmology and Foregrounds from BICEP2 and Keck Array Cosmic Microwave Background Data with Inclusion of 95 GHz Band. *Phys. Rev. Lett.* **2016**, *116*, 031302.
36. Barbon, J.L.F.; Espinosa, J.R. On the Naturalness of Higgs Inflation. *Phys. Rev. D* **2009**, *79*, 081302.
37. Burgess, C.P.; Lee, H.M.; Trott, M. On Higgs Inflation and Naturalness. *J. High Energy Phys.* **2010**, *2010*, 007.
38. Kehagias, A.; Dizgah, A.M.; Riotto, A. Remarks on the Starobinsky model of inflation and its descendants. *Phys. Rev. D* **2014**, *89*, 043527.
39. Kawasaki, M.; Yamaguchi, M.; Yanagida, T. Natural chaotic inflation in supergravity. *Phys. Rev. Lett.* **2000**, *85*, 3572.
40. Brax, P.; Martin, J. Shift symmetry and inflation in supergravity. *Phys. Rev. D* **2005**, *72*, 023518.
41. Antusch, S.; Dutta, K.; Kostka, P.M. SUGRA Hybrid Inflation with Shift Symmetry. *Phys. Lett. B* **2009**, *677*, 221–225.
42. Kallosh, R.; Linde, A.; Rube, T. General inflaton potentials in supergravity. *Phys. Rev. D* **2011**, *83*, 043507.
43. Li, T.; Li, Z.; Nanopoulos, D.V. Supergravity Inflation with Broken Shift Symmetry and Large Tensor-to-Scalar Ratio. *J. Cosmol. Astropart. Phys.* **2014**, *2014*, 028.

44. Harigaya, K.; Yanagida, T.T. Discovery of Large Scale Tensor Mode and Chaotic Inflation in Supergravity. *Phys. Lett. B* **2014**, *734*, 13–16.
45. Mazumdar, A.; Noumi, T.; Yamaguchi, M. Dynamical breaking of shift-symmetry in supergravity-based inflation. *Phys. Rev. D* **2014**, *90*, 043519.
46. Pallis, C.; Shafi, Q. From Hybrid to Quadratic Inflation With High-Scale Supersymmetry Breaking. *Phys. Lett. B* **2014**, *736*, 261–266.
47. Ben-Dayan, I.; Einhorn, M.B. Supergravity Higgs Inflation and Shift Symmetry in Electroweak Theory. *J. Cosmol. Astropart. Phys.* **2010**, *2010*, 2.
48. Lazarides, G.; Pallis, C. Shift Symmetry and Higgs Inflation in Supergravity with Observable Gravitational Waves. *J. High Energy Phys.* **2015**, *2015*, 114.
49. Pallis, C.; Toumbas, N. Starobinsky-type inflation with products of Kähler manifolds. *J. Cosmol. Astropart. Phys.* **2016**, *2016*, 015.
50. Pallis, C.; Toumbas, N. Starobinsky Inflation: From Non-SUSY To SUGRA Realizations. *Adv. High Energy Phys.* **2017**, *2017*, 6759267.
51. Pallis, C. Observable Gravitational Waves From Higgs Inflation in SUGRA. *PoS EPS-HEP* **2017**, *2017*, 047.
52. Hamaguchi, K. Cosmological baryon asymmetry and neutrinos: Baryogenesis via leptogenesis in supersymmetric theories. *Arxiv* **2002**, arXiv:hep-ph/0212305.
53. Buchmüller, W.; Peccei, R.D.; Yanagida, T. Leptogenesis as the origin of matter. *Ann. Rev. Nucl. Part. Sci.* **2005**, *55*, 311–355.
54. Pallis, C. Linking Starobinsky-Type Inflation in no-Scale Supergravity to MSSM. *J. Cosmol. Astropart. Phys.* **2014**, *2014*, 024; Erratum in **2017**, *2017*, 01.
55. Pallis, C.; Shafi, Q. Non-Minimal Chaotic Inflation, Peccei-Quinn Phase Transition and non-Thermal Leptogenesis. *Phys. Rev. D* **2012**, *86*, 023523.
56. Ade, P.A.R.; Aghanim, N.; Arnaud, M.; Ashdown, M.; Aumont, J.; Baccigalupi, C.; Banday, A.J.; Barreiro, R.B.; Bartlett, J.G.; Bartolo, N. Planck 2015 results. XIII. Cosmological parameters. *Astron. Astrophys.* **2016**, *594*, A13.
57. Lazarides, G.; Shafi, Q. Origin of matter in the inflationary cosmology. *Phys. Lett. B* **1991**, *258*, 305.
58. Kumekawa, K.; Moroi, T.; Yanagida, T. Flat potential for inflaton with a discrete R invariance in supergravity. *Prog. Theor. Phys.* **1994**, *92*, 437–447.
59. Lazarides, G.; Schaefer, R.K.; Shafi, Q. Supersymmetric inflation with constraints on superheavy neutrino masses. *Phys. Rev. D* **1997**, *56*, 1324.
60. Khlopov, M.Y.; Linde, A.D. Is It Easy to Save the Gravitino? *Phys. Lett. B* **1984**, *138*, 265–268.
61. Ellis, J.; Kim, J.E.; Nanopoulos, D.V. Cosmological Gravitino Regeneration and Decay. *Phys. Lett. B* **1984**, *145*, 181–186.
62. Bolz, M.; Brandenburg, A.; Buchmüller, W. Thermal production of gravitinos. *Nucl. Phys. B* **2001**, *606*, 518–544; Erratum in **2008**, *790*, 336.
63. Pradler, J.; Steffen, F.D. Thermal gravitino production and collider tests of leptogenesis. *Phys. Rev. D* **2007**, *75*, 023509.
64. Cyburt, R.H.; Ellis, J.; Fields, B.D.; Olive, K.A. Updated nucleosynthesis constraints on unstable relic particles. *Phys. Rev. D* **2003**, *67*, 103521.
65. Kawasaki, M.; Kohri, K.; Moroi, T. Hadronic decay of late - decaying particles and Big-Bang Nucleosynthesis. *Phys. Lett. B* **2005**, *625*, 7–12.
66. Kawasaki, M.; Kohri, K.; Moroi, T. Big-Bang nucleosynthesis and hadronic decay of long-lived massive particles. *Phys. Rev. D* **2005**, *71*, 083502.
67. Ellis, J.R.; Olive, K.A.; Vangioni, E. The Effects of unstable particles on light-element abundances: Lithium versus deuterium and He-3. *Phys. Lett. B* **2005**, *619*, 30–42.
68. Ellis, J.; Garcia, M.A.G.; Nanopoulos, D.V.; Olive, K.A.; Peloso, M. Post-Inflationary Gravitino Production Revisited. *J. Cosmol. Astropart. Phys.* **2016**, *2016*, 008.
69. Ema, Y.; Mukaida, K.; Nakayama, K.; Terada, T. Nonthermal Gravitino Production after Large Field Inflation. *J. High Energy Phys.* **2016**, *2016*, 184.
70. Forero, D.V.; Tortola, M.; Valle, J.W.F. Neutrino oscillations refitted. *Phys. Rev. D* **2014**, *90*, 093006.
71. Gonzalez-Garcia, M.C.; Maltoni, M.; Schwetz, T. Updated fit to three neutrino mixing: Status of leptonic CP violation. *J. High Energy Phys.* **2014**, *2014*, 052.

72. Capozzi, F.; Lisi, E.; Marrone, A.; Montanino, D.; Palazzo, A. Neutrino masses and mixings: Status of known and unknown 3ν parameters. *Nucl. Phys. B* **2016**, *908*, 218–234.
73. Dvali, G.R.; Lazarides, G.; Shafi, Q. Mu problem and hybrid inflation in supersymmetric SU(2)-L x SU(2)-R x U(1)-(B-L). *Phys. Lett. B* **1998**, *424*, 259–264.
74. Endo, M.; Takahashi, F.; Yanagida, T.T. Inflaton Decay in Supergravity. *Phys. Rev. D* **2007**, *76*, 083509.
75. Einhorn, M.B.; Jones, D.R.T. Inflation with Non-minimal Gravitational Couplings in Supergravity. *J. High Energy Phys.* **2010**, *2010*, 26.
76. Lee, H.M. Chaotic inflation in Jordan frame supergravity. *J. Cosmol. Astropart. Phys.* **2010**, *2010*, 003.
77. Ferrara, S.; Kallosh, R.; Linde, A.; Marrani, A.; Van Proeyen, A. Superconformal Symmetry, NMSSM, and Inflation. *Phys. Rev. D* **2011**, *83*, 025008.
78. Pallis, C.; Toumbas, N. Non-Minimal Sneutrino Inflation, Peccei-Quinn Phase Transition and non-Thermal Leptogenesis. *J. Cosmol. Astropart. Phys.* **2011**, *2011*, 019.
79. Lopes Cardoso, G.; Lüst, D.; Mohaupt, T. Moduli spaces and target space duality symmetries in (0,2) Z(N) orbifold theories with continuous Wilson lines. *Nucl. Phys. B* **1994**, *432*, 68–108.
80. Antoniadis, I.; Gava, E.; Narain, K.S.; Taylor, T.R. Effective mu term in superstring theory. *Nucl. Phys. B* **1994**, *432*, 187–204.
81. Pallis, C. Reconciling Induced-Gravity Inflation in Supergravity With The Planck 2013 & BICEP2 Results. *J. Cosmol. Astropart. Phys.* **2014**, *2014*, 058.
82. Pallis, C. Induced-Gravity Inflation in Supergravity Confronted with Planck 2015 & BICEP2/Keck Array. *Arxiv* **2015**, arXiv:1506.03731
83. Pallis, C.; Shafi, Q. Gravity Waves From Non-Minimal Quadratic Inflation. *J. Cosmol. Astropart. Phys.* **2015**, *2015*, 023.
84. Kallosh, R.; Linde, A.; Roest, D. Superconformal Inflationary α-Attractors. *J. High Energy Phys.* **2013**, *2013*, 198.
85. Kallosh, R.; Linde, A.; Roest, D. Large field inflation and double α-attractors. *J. High Energy Phys.* **2014**, *2014*, 1–22.
86. Boubekeur, L.; Lyth, D. Hilltop inflation. *J. Cosmol. Astropart. Phys.* **2005**, *07*, 010.
87. Armillis, R.; Pallis, C. Implementing Hilltop F-term Hybrid Inflation in Supergravity. In *Recent Advances in Cosmology*; Travena, A., Soren, B., Eds.; Nova Science Publishers, Inc.: New York, NY, USA, 2013; pp. 159–192.
88. Garbrecht, B.; Pallis, C.; Pilaftsis, A. Anatomy of F(D)-Term Hybrid Inflation. *J. High Energy Phys.* **2006**, *2006*, 038.
89. Pallis, C.; Shafi, Q. Update on Minimal Supersymmetric Hybrid Inflation in Light of PLANCK. *Phys. Lett. B* **2013**, *725*, 327–333.
90. Civiletti, M.; Pallis, C.; Shafi, Q. Upper Bound on the Tensor-to-Scalar Ratio in GUT-Scale Supersymmetric Hybrid Inflation. *Phys. Lett. B* **2014**, *733*, 276–282.
91. Antusch, S.; Spinrath, M. Quark and lepton masses at the GUT scale including SUSY threshold corrections. *Phys. Rev. D* **2008**, *78*, 075020.
92. Coleman, S.R.; Weinberg, E.J. Radiative Corrections as the Origin of Spontaneous Symmetry Breaking. *Phys. Rev. D* **1973**, *7*, 1888–1910.
93. Lyth, D.H.; Riotto, A. Particle physics models of inflation and the cosmological density perturbation. *Phys. Rept.* **1999**, *314*, 1–146.
94. Lazarides, G. Basics of inflationary cosmology. *J. Phys. Conf. Ser.* **2006**, *53*, 528–550.
95. Martin, J.; Ringeval, C.; Vennin, V. Encyclopedia Inflationaris. *Phys. Dark Universe* **2014**, *5*, 75–235.
96. Wolfram Research. Available online: http://functions.wolfram.com (accessed on 4 January 2018).
97. Wu, W.L.K.; Ade, P.A.R.; Ahmed, Z.; Alexander, K.D.; Amiri, M.; Barkats, D.; Benton, S.J.; Bischoff, C.A.; Bock, J.J.; Bowens-Rubin, R.; et al. Initial Performance of BICEP3: A Degree Angular Scale 95 GHz Band Polarimeter. *J. Low. Temp. Phys.* **2016**, *184*, 765–771.
98. Andre, P.; Baccigalupi, C.; Barbosa, D.; Bartlett, J.; Bartolo, N.; Battistelli, E.; Battye, R.; Bendo, G.; Bernard, J.-P.; Bersanelli, M.; et al. PRISM (Polarized Radiation Imaging and Spectroscopy Mission): A White Paper on the Ultimate Polarimetric Spectro-Imaging of the Microwave and Far-Infrared Sky. *Arxiv* **2013**. arXiv:1306.2259
99. Matsumura, T.; Akiba, Y.; Borril, J.; Chinone, Y.; Dobbs, M.; Fuke, H.; Ghribi, A.; Hasegawa, M.; Hattori, K.; Hattori, M. Mission design of LiteBIRD. *J. Low. Temp. Phys.* **2014**, *176*, 733–740.

100. Martin, S.P. A Supersymmetry primer. *Adv. Ser. Direct. High Energy Phys.* **2010**, *21*, 1–153.
101. Athron, P.; Balazs, C.; Bringmann, T.; Buckley, A.; Chrzaszcz, M.; Conrad, J.; Cornell, J.M.; Dal, L.A.; Edsjo, J.; Farmer, B.; et al. Global fits of GUT-scale SUSY models with GAMBIT. *Eur. Phys. J. C* **2017**, *77*, 824.
102. Buchmüller, W.; Dudas, E.; Heurtier, L.; Wieck, C. Large-Field Inflation and Supersymmetry Breaking. *J. High Energy Phys.* **2014**, *2014*, 53.
103. Ellis, J.R.; Garcia, M.; Nanopoulos, D.; Olive, K.A. Phenomenological Aspects of No-Scale Inflation Models. *J. Cosmol. Astropart. Phys.* **2015**, *2015*, 003.
104. Nilles, H.P. Supersymmetry, Supergravity and Particle Physics. *Phys. Rept.* **1984**, *110*, 1–162.
105. Pallis, C. Kination-dominated reheating and cold dark matter abundance. *Nucl. Phys. B* **2006**, *751* 129–159.
106. Şenoğuz, V.N. Non-thermal leptogenesis with strongly hierarchical right handed neutrinos. *Phys. Rev. D* **2007**, *76*, 013005.
107. Feng, J.L.; Rajaraman, A.; Takayama, F. SuperWIMP dark matter signals from the early universe. *Phys. Rev. D* **2003**, *68*, 063504.
108. Steffen, F.D. Gravitino dark matter and cosmological constraints. *J. Cosmol. Astropart. Phys.* **2006**, *2006*, 001.
109. Kanzaki, T.; Kawasaki, M.; Kohri, K.; Moroi, T. Cosmological constraints on gravitino LSP scenario with sneutrino NLSP. *Phys. Rev. D* **2007**, *75*, 025011.
110. Roszkowski, L.; Trojanowski, S.; Turzynski, K.; Jedamzik, K. Gravitino dark matter with constraints from Higgs boson mass and sneutrino decays. *J. High Energy Phys.* **2013**, *2013*, 13.
111. Dine, M.; Kitano, R.; Morisse, A.; Shirman, Y. Moduli decays and gravitinos. *Phys. Rev. D* **2006**, *73*, 123518.
112. Kitano, R. Gravitational Gauge Mediation. *Phys. Lett. B* **2006**, *641*, 203–207.
113. Evans, J.L.; Garcia, M.A.G.; Olive, K.A. The Moduli and Gravitino (non)-Problems in Models with Strongly Stabilized Moduli. *J. Cosmol. Astropart. Phys.* **2014**, *2014*, 022.
114. Flanz, M.; Paschos, E.A.; Sarkar, U. Baryogenesis from a lepton asymmetric universe. *Phys. Lett. B* **1995**, *345*, 248–252.
115. Covi, L.; Roulet, E.; Vissani, F. CP violating decays in leptogenesis scenario. *Phys. Lett. B* **1996**, *384*, 169–174.
116. Flanz, M.; Paschos, E.A.; Sarkar, U.; Weiss, J. Baryogenesis through mixing of heavy Majorana neutrinos. *Phys. Lett. B* **1996**, *389*, 693–699.
117. Armillis, R.; Lazarides, G.; Pallis, C. Inflation, leptogenesis, and Yukawa quasiunification within a supersymmetric left-right model. *Phys. Rev. D* **2014**, *89*, 065032.
118. Antusch, S.; Kersten, J.; Lindner, M.; Ratz, M. Running neutrino masses, mixings and CP phases: Analytical results and phenomenological consequences. *Nucl. Phys. B* **2003**, *674*, 401–433.
119. Lazarides, G.; Shafi, Q. R symmetry in minimal supersymmetry standard model and beyond with several consequences. *Phys. Rev. D* **1998**, *58*, 071702.
120. Karagiannakis, N.; Lazarides, G.; Pallis, C. Cold Dark Matter and Higgs Mass in the Constrained Minimal Supersymmetric Standard Model with Generalized Yukawa Quasi-Unification. *Int. J. Mod. Phys. A* **2013**, *28*, 1330048.